Electroporation optimization for AML cell lines and CRISPR-Cas9-mediated knockout of immune-related genes in AML

Dissertation

zur Erlangung des akademischen Grades eines

Doktors der Medizin (Dr. med.)

an der

Medizinischen Fakultät der Universität Hamburg

vorgelegt von

Rui Lu

aus

Anhui, China

2026

Betreuer:in / Gutachter:in der Dissertation: PD Dr. Jasmin Wellbrock

Gutachter:in der Dissertation: Prof. Dr. Volkmar Müller

Vorsitz der Prüfungskommission: Prof. Dr. Volkmar Müller

Mitglied der Prüfungskommission: PD Dr. Kerstin Cornils

Mitglied der Prüfungskommission: Prof. Dr. Arne Hansen

Datum der mündlichen Prüfung: 30.06.2026

1. Objectives

Acute myeloid leukemia (AML) is a malignant blood cancer caused by the abnormal proliferation of immature bone marrow cells. Approximately half of patients fail to attain remission after initial treatment (Mohamed Jiffry et al., 2023). Immunotherapy helps the immune system recognize and attack cancer cells, preventing the tumors from evading immune detection. It can cause fewer side effects than chemotherapy, and improve long-term survival in many cancers (Ahvati et al., 2025). Immunotherapy is now being tested in AML, including checkpoint inhibitors against CTLA-4 or PD-1 and CAR-T therapies targeting antigens on AML blasts (Short et al., 2018). The success of these approaches depends on the identification of immune-related genes that play meaningful roles in AML pathogenesis. Molecules such as PVR, PVRL2, CD48, CD111, CD47, and CD39 are of particular interest. Extensive literature, together with our laboratory's preliminary findings, indicates that their relevance to AML pathobiology should be investigated through direct functional studies (Brauneck et al., 2022, Wang et al., 2021a, Wang et al., 2021b, Aroua et al., 2020). AML cell lines, as controllable and easy to use in vitro models, are suitable for such validation. But this requires efficient gene knockout techniques that are reproducible and suitable for existing laboratory equipment. AML cell lines are suspension cells, they are more difficult to transfect and transduce than adherent cells (Cheng et al., 2022, Richter et al., 2021). Conventional transfection approaches frequently result in poor efficiency when applied to suspension leukemia cell lines (Agarwal and Tyner, 2016). To overcome the difficulty of transfecting suspension cell lines, electroporation could be the only technique consistently capable of introducing various molecules into non-adherent cells with high efficiency (Vadeikiene et al., 2022, Agarwal and Tyner, 2016). The CRISPR-Cas9 system is famous for its ability to edit genes (Hryhorowicz et al., 2017). It has greatly expanded the research field for understanding and treating AML, because it can edit genes related to the disease quickly and precisely (Neldeborg et al., 2023, Xu et al., 2023).

Therefore, this study had the following objectives: 1. Can electroporation conditions be systematically optimized to achieve high transfection efficiency and cell viability in AML cell lines? 2. Can optimized electroporation enable stable CRISPR-Cas9 mediated knockout of immune-related genes, such as PVR, PVRL2, CD48, CD111, CD47 and CD39, including the establishment of single knockouts of these individual genes, double knockouts with PVR, PVRL2, and triple knockouts combining PVR, PVRL2 with another gene of interest?

2. Introduction

2.1 Acute myeloid leukemia (AML) background

Acute myeloid leukemia (AML) is a serious form of malignant bone marrow cancer in which immature myeloid cells multiply abnormally and fail to develop properly (Shallis et al., 2019, Nguyen et al., 2024). Among adults, AML is the most common type of acute leukemia. In 2023, there were approximately 20,380 new cases and 11,310 related deaths in the United States. The disease occurs at a rate of 4.3 per 100,000 people each year, and is mainly seen in older adults. Most diagnoses occur at the age of 68 (Shallis et al., 2019, Wysota et al., 2024). The standard induction treatment often uses high doses of cytarabine with other drugs. However, a significant number of patients either experience a relapse or fail to respond to treatment, highlighting the need for improved treatment strategies (Bruck et al., 2020). Recently, more studies of the genetic background of AML have led to the development of new targeted therapies. However, patients' overall survival rates are still not high (Pelcovits and Niroula, 2020). Therefore, more relevant research needs to be conducted to promote the treatment of AML.

Immunotherapy is now widely used in cancer treatment. It can give patients long-lasting effects, cause fewer side effects, and improve patients' survival and quality of life (Mohammadian Gol et al., 2023, Wang et al., 2024). According to Zhang et al., cancer immunotherapy mechanisms can be divided into five kinds. They are immune checkpoint modulation, oncolytic virus treatment, cancer vaccines, cytokine-based therapies, and adoptive cell transfer (Zhang and Zhang, 2020, Kciuk et al., 2023). AML often tends to relapse because it can avoid immune detection e.g. through immune checkpoint expression, weakening the antigen presentation, and altering the tumor microenvironment to create an immunosuppressive state. Over time, this leads to T cell exhaustion (Soleimani Samarkhazan et al., 2025, Bareke et al., 2021). Tumor cells can escape from immune surveillance by expressing immune checkpoint ligands like PD-L1 and Gal9, which bind to the corresponding immune checkpoint receptors on T cells thereby preventing them from working properly. By blocking these proteins, immune checkpoint inhibitors can reactivate T cell function, allowing them to attack cancer cells effectively (Witkowska and Smolewski, 2018, Kciuk et al., 2023).

In recent years, our research group has conducted extensive research on the emerging immune target TIGIT (T cell immunoglobulin and immunoreceptor tyrosine-based inhibitory motif (ITIM)). We have found that AML cell lines and AML patient samples

show high levels of TIGIT ligands PVR and PVRL2. AML patients showing higher expression levels tend to have a poorer prognosis. Blocking the PVR/PVRL2/TIGIT pathway could be a potential treatment for AML in the future (Stamm et al., 2018a, Stamm et al., 2018b). Blocking TIGIT could make anti-CD47 treatment more effective at promoting phagocytosis, in both AML cell lines and primary AML cells (Brauneck et al., 2022). In a leukemia mouse model, spleen-infiltrating regulatory $CD4^+$ T cells exhibited an effector memory phenotype. These cells had high levels of checkpoint molecules such as TIGIT, PD-1, and OX40, and also the ectoenzymes CD39 and CD73 (Kruger et al., 2024). The TIGIT axis and the CD39/CD73 purinergic pathway were markedly expressed in immune cells derived from bone metastases. Blocking TIGIT and CD39 could enhance PBMC-mediated lysis of tumor cells (Brauneck et al., 2025). Moreover, blocking TIGIT and CD39 or A2AR boosted NK-92 cell mediated killing of AML cells (Brauneck et al., 2021). The advancement of cancer immunotherapy may rely on the use of combination treatment strategies (Esfahani et al., 2020, Stahl and Goldberg, 2019). Therefore, we were not only interested in studying the role of a series of immune-related genes in the development of leukemia, but we also aimed to combine them with TIGIT blockade. We planned to generate a triple knockout cell line by deleting PVR, PVRL2, and another protein of interest, in order to compare it with single and double knockout variants.

2.2 Immune related genes in AML

Immune checkpoint molecules control the activation and suppression of immune cells. CTLA-4 and PD-1 are well known immune checkpoints that play a key role in cancer immunotherapy. Recently, the poliovirus receptor (PVR)-like family, including DNAM-1, TIGIT (T cell immunoglobulin and immunoreceptor tyrosine-based inhibitory motif (ITIM)), CD96, and CD112R, has been identified as a new group of receptors. These receptors interact with PVR (CD155), PVRL2 (CD112), PVRL3 (CD113) and PVRL1 (CD111) to control T cells and NK cells activities (Wu et al., 2021, Kaito et al., 2024). The interaction between TIGIT and PVR is significantly stronger than that observed with PVRL2 or CD113 (Jantz-Naeem et al., 2023, Mei et al., 2020). TIGIT is frequently overexpressed in both solid tumors and hematologic malignancies, including melanoma, gastric cancer, acute myeloid leukemia, and multiple myeloma. In tumors, elevated TIGIT signaling is associated with impaired function of cytotoxic T cells and NK cells.

Elevated TIGIT expression suppresses immune cell activity, weakening antitumor responses and facilitating tumor immune escape and disease progression (Cai et al., 2023, Cheng et al., 2024).

In immune cells, inhibitory signaling mediated by TIGIT primarily occurs through its interactions with PVR and PVRL2. PVR and PVRL2 belong to the nectin and nectin-like group of the immunoglobulin superfamily and serve as poliovirus receptors. Increased PVR expression has been observed in various cancers, such as pancreatic, lung, soft tissue tumors and melanoma. PVRL2 can be found in endothelial, epithelial, and fibroblast cells. Its elevated expression has been linked to tumor formation and metastatic potential (Meggyes et al., 2022, Lupo and Matosevic, 2020). The binding of TIGIT with PVR reduces T cell activation and weakens NK cell cytotoxicity, leading to decreased killing of tumor cells (Wu et al., 2021). Inhibiting the TIGIT/PVR signaling pathway rescues exhausted $CD8^+$ T cells and strengthens their antitumor efficacy in cervical cancer (Liu et al., 2022b). Increased PVR expression predicts a poor outcome in patients receiving PD-1/PD-L1 blockade (Jiang et al., 2022). Dual inhibition of PVR together with PD-1/PD-L1 can significantly improve immune based treatment responses (Chu et al., 2023). Seel et al. reported that AML patients with poor prognosis often show increased expression of PVR and PVRL2 together with reduced CD86 levels. The elevated PVR and PVRL2 on AML blasts may contribute to NK cell exhaustion, which could be improved by NK-92 adoptive transfer together with TIGIT inhibition (Seel et al., 2024). These findings all indicate that PVR and PVRL2 could play a significant role in tumor progression and immune modulation.

CD111 is also a member of the nectin and nectin-like family of immunoglobulin superfamily receptors. Its major roles involve promoting cell adhesion, functioning as an immune receptor, and acting as a receptor for viruses (Romanczyk and Pryczynicz, 2025, Hegazy et al., 2022). CD111 is highly expressed in medulloblastoma, colorectal cancer cells, hepatocellular carcinoma and breast cancer (Friedman et al., 2016, Tampakis et al., 2019, Wang et al., 2022, Martin et al., 2013). CD111 functions as a CD96 ligand, participating in the control of NK cell and T cell responses (Wu et al., 2021). Higher levels of CD111 were found on CD34+ cells from mobilized peripheral blood than from cord blood, and CD34+/CD38+ cells express more CD111 than CD34+/CD38− cells (Belaaloui et al., 2003). To date, the role of CD111 in hematologic malignancies, such as leukemia, has not been reported.

CD48 is a part of the signaling lymphocyte activation marker (SLAM) family, a group of molecules that are essential for immune cell regulation and are involved in processes like tolerance, humoral immunity, autoimmunity and cytotoxicity (Cannons et al., 2011). CD48 is widely expressed on most hematopoietic cells under normal condition. Soluble CD48 is present in human serum and plasma, and its levels are elevated in patients affected by leukemia (McArdel et al., 2016). Hosen et al. first found that CD48 is highly expressed on multiple myeloma (MM) plasma cells, and treatment with an anti-CD48 monoclonal antibody effectively inhibited MM cell growth in mice without harming normal CD34(+) haematopoietic stem/progenitor cells, indicating that CD48 may act as a therapeutic target for treating MM (Hosen et al., 2012). In hepatocellular carcinoma (HCC), inhibition of the CD48 receptor 2B4 on NK cells significantly reduced monocyte-induced impairment of NK cell function. (Wu et al., 2013). As the primary receptor of GDF15 in immune cells, CD48 mediates the enhancement of Treg cell function in HCC, highlighting its importance in tumor related immunosuppression (Wang et al., 2021c).

CD39 (ectonucleoside triphosphate diphosphohydrolase 1) is an ectoenzyme that, together with CD73, participates in a metabolic cascade converting ATP (adenosine triphosphate) into ADP (adenosine diphosphate) and cAMP (cyclic adenosine monophosphate), eventually resulting in the production of extracellular adenosine. Many studies have shown that extracellular adenosine is involved in the immune suppression (Timperi and Barnaba, 2021, Ohta and Sitkovsky, 2001, Huang et al., 1997). Elevated CD39 expression has been reported in various human cancers, such as lung cancer, ovarian cancer, thyroid cancer, lymphoma, colon cancer, sarcoma, melanoma, chronic lymphocytic leukemia, pancreatic cancer, and testicular cancer. Moreover, high expression of CD39 in tumors tends to be associated with poorer prognosis (Bastid et al., 2015, Hayes et al., 2015, Moesta et al., 2020, Häusler et al., 2011, Timperi and Barnaba, 2021). According to Feng et al., CD39 expression enhances tumor cell proliferation by breaking down extracellular ATP, and inhibition of its activity may be a potential therapeutic approach (Feng et al., 2011). Recent research increasingly supports the idea that adenosine-dependent immune suppression represents a key pathway of tumor immune escape. Inhibiting CD39 can strengthen antitumor immune responses by reducing adenosine production and increasing extracellular ATP levels. Combining CD39 inhibition with other targets in the adenosine pathway, immune checkpoint

inhibitors (such as PD-1, TIM-3,or CTLA-4) has shown cooperative antitumor effects in both experimental models and clinical research (Guo et al., 2022).

Belonging to the immunoglobulin superfamily, CD47 is a transmembrane protein extensively distributed on normal hematopoietic cell membranes. CD47 binds to signal-regulatory protein alpha (SIRPα) to inhibit macrophage-mediated clearance of red blood cells and acts as a key immune checkpoint that delivers a “don’t eat me” signal (Ahvati et al., 2025, Qiu et al., 2021). High levels of CD47 are commonly found in many cancers. It is highly expressed in solid tumors, such as nonsmall cell lung cancer (Catalán et al., 2020) and hepatocellular carcinoma (Abd El-Fattah and Selim, 2022), and also in blood cancers like leukemia and multiple myeloma (MM), where it predicts poor prognosis (Li et al., 2024). Multiple clinical studies are investigating antibodies against the checkpoint protein CD47, among which magrolimab is currently the most advanced in development (Montero and Isenberg, 2023). Although CD47 blockade shows promising anti-tumor potential, its broad expression on red blood cells and platelets leads to safety concerns such as anemia. Recent studies aim to develop selective CD47 antibodies that maintain anti-tumor activity while minimizing hematologic toxicity (Liu et al., 2024). Therefore, knocking out CD47 in AML cell lines allows a more direct evaluation of its key role in immune evasion and growth of leukemic cells, providing a theoretical basis for future drug development.

2.3 Gene editing in AML cells

To achieve stable gene knockout, viral transfection, nonviral transfection, or a combination of both can be used (Chong et al., 2021). Compared with viral transfection, nonviral gene delivery is safer and avoids strong immune responses. Among various nonviral methods, electroporation is the most effective and well-developed technique. By using short electrical pulses, a temporary increase in cell membrane permeability can be achieved. This could allow DNA, mRNA and proteins to enter various cell types more easily and achieve higher levels of gene expression. Its safety, flexibility, and scalability make electroporation a valuable method for delivering genes and manufacturing therapeutic cells (Young and Dean, 2015, Timmins et al., 2021). The low efficiency of transfection or transduction in AML cells remains a major challenge in research and therapy (Cheng et al., 2022, Richter et al., 2021). Because acute myeloid leukemia cells are non-adherent, their transfection efficiency is generally lower compared with adherent

cells (Harris and Elmer, 2021). Recently, the use of electroporation in leukemia cell lines has become an increasingly important topic in cancer research (Vadeikienė et al., 2022).

Electroporation systems, for instance Lonza's Nucleofector and Thermo Fisher Neon™ Transfection System, offer high transfection efficiency and are widely adopted in experimental applications. However, both Lonza's Nucleofector and the Neon™ Transfection System depend on proprietary electroporation kits and buffers, and the high cost of these consumables restricts their routine use in the laboratory (Chicaybam et al., 2016, Brees and Fransen, 2014). In this study, we chose to use the Bio-Rad Gene Pulser Xcell electroporation system because it is more affordable and easier to adjust for different experimental setups. The machine supports square-wave pulses, and both the voltage and pulse duration can be modified depending on the cell type. We used the square wave pulse for electroporation, because this wave form has been shown to be optimal for mammalian cell transfection (Hyder et al., 2020). When performing electroporation on different cell types, it is necessary to optimize experimental parameters beforehand. Electric field strength, pulse number and duration, and electroporation buffer are all important parameters to adjust when optimizing electroporation conditions (Bajwa et al., 2023, Cemazar et al., 2002).

2.4 CRISPR-Cas9 technology

CRISPR-Cas9 is a gene editing tool from the immune system of bacteria that allows scientists to edit genes efficiently and accurately. CRISPR-Cas9 uses the guide RNA and Cas9 protein to find and cut specific DNA sequences. Cas9 is guided by the guide RNA to the specific DNA sequence and then cuts it (Janik et al., 2020).

CRISPR-Cas9 could play an important role in enhancing the application of immunotherapy in cancer treatment. Feng et al. found that CRISPR-Cas9 knockout of CDK11 reduces osteosarcoma cell growth, survival, migration, and invasion, suggesting that CDK11 might be a potential therapeutic target for this cancer (Feng et al., 2015). Zhang et al. showed that CRISPR-Cas9 can efficiently delete LAG-3 in CAR-T cells without damaging the cells. And the modified CAR-T cells still showed antitumor effects in vitro and in mouse models. These results suggest that gene editing could be a useful tool for targeting immune checkpoints in CAR-T therapy (Zhang et al., 2017). Bexte et al. used CRISPR-Cas9 to delete NKG2A from primary NK cells. After editing, the edited

cells showed better antitumor ability to attack multiple myeloma cells. Cytokine secretion was not changed, suggesting gene editing could improve NK cell immunotherapy (Bexte et al., 2022).

Using CRISPR-Cas9 in the form of ribonucleoprotein (RNP) complexes is considered a practical and efficient way to edit genomes. The editing process can start soon after the complex enters the cell, which helps to achieve high on-target efficiency, promotes cell survival and reduces unwanted off-target effects (Behr et al., 2021). Since both the Cas9 protein and the guide RNA stay in the cell only for a short time, the chance of triggering an immune response is low. Electroporation has become the dominant technique used to transfer RNP into target cells for therapeutic purposes (Tyumentseva et al., 2023, Cheng et al., 2022). Therefore, exploring and optimizing effective and reproducible CRISPR-Cas9 mediated electroporation methods is essential for investigating novel therapeutic targets for AML.

3 Materials and Methods

3.1 Cell lines and culture medium

Table 1.

AML cell line	Specific medium	Supplements
Molm13	RPMI 1640 medium	10% fetal bovine serum (FBS)
TF-1	RPMI 1640 medium	20% FBS and 2 ng/ml GM-CSF
OCI-AML5	alpha-MEM medium	20% FBS and 2 ng/ml GM-CSF
KG-1	RPMI 1640 medium	10% FBS
UKE-1	IMDM medium	10% FBS, 10% horse serum, 1 μM hydrocortisone, 500 μL

All cells were cultured at 37 °C with 5% CO_2.

3.2 Materials

Equipment:

Gene Pulser Xcell Electroporation System (Bio-Rad), Eppendorf 5424 centrifuge, Eppendorf Thermo Mixer C, Vi-CELL XR cell counter (Beckman Coulter, Brea, CA, USA), Fortessa flow cytometer (BD Biosciences), FACSAria IIIu flow cytometer (BD Biosciences).

Reagents:

Invitrogen™ TrueGuide Synthetic gRNA (PVR, human) CRISPR923263_SGM (Thermo Fisher Scientific), Invitrogen™ TrueGuide Synthetic gRNA (PVRL2, human) CRISPR688341_SGM (Thermo Fisher Scientific), Invitrogen™ TrueGuide Synthetic gRNA (CD39, human) CRISPR850040_SGM (Thermo Fisher Scientific), Invitrogen™ TrueGuide Synthetic gRNA (CD47, human) CRISPR1036169_SGM (Thermo Fisher Scientific), Invitrogen™ TrueGuide Synthetic gRNA (CD48, human) CRISPR900163_SGM (Thermo Fisher Scientific), Invitrogen™ TrueGuide Synthetic gRNA (CD111, human) CRISPR933570_SGM (Thermo Fisher Scientific), Invitrogen™ TrueCut™ Cas9 Protein v2, 100 μg (Thermo Fisher Scientific,

Cat:A36498), Opti-MEM® I Reduced Serum Medium (Gibco, Thermo Fisher Scientific, Cat:31985-062), GFP mRNA was transcribed in vitro from a pJET-GFP plasmid (constructed in-house; vector from ThermoFisher) kindly provided by Prof. Boris Fehse, peqGOLD Blood & Tissue DNA Mini Kit, Natriumazid 10 % (MORPHISTO, REF: 13553.00100), UltraPure™ 0,5 M EDTA, pH 8,0, 100 ml (Invitrogen™ , REF:15575-038), POLYSUCROSE 400 SOLUTION unit 500ml (BIOCLOT), CellTracker™ Green CMFDA (Thermo Fisher Scientific, Invitrogen)，Dynabeads™ humaner T-Activator CD3/CD28 zur Expansion und Aktivierung von T-Zellen (Gibco, Thermo Fisher Scientific, Cat:11132D), Human GM-CSF Recombinant Protein, PeproTech® (Gibco, Thermo Fisher Scientific, Cat:300-03-50UG), 7-AAD Viability Staining Solution (BioLegend, Cat: 420404), FcR Blocking Reagent, human (Miltenyi Biotec, Cat:130-059-901), RPMI 1640 medium (Gibco, Thermo Fisher Scientific), alpha-MEM medium (Gibco, Thermo Fisher Scientific), IMDM medium (Gibco, Thermo Fisher Scientific).

Consumables

Gene Pulser/Micro Pulser Electroporation Cuvettes, 0.2 cm gap #1652086 (Bio-Rad), 24-well plate, 96-well plate.

Table 2. SgRNAs

sgRNA ID	Target locus (GRCh38)	Strand	Target DNA sequence (5'–3')	PAM
sgRNA PVR	Chr.19: 44647393-44647415	Forward	CGTTTGGACTCCGAATAGCT	GGG
sgRNA PVRL2	Chr.19: 44865284-44865306	Forward	GCGAGTTCAAGTGCTACCCG	AGG
sgRNA CD39	Chr.10: 95842445-95842467	Forward	CAAGAGACACCCGTTTACCT	GGG
sgRNA CD47	Chr.3: 108080169-108080191	Forward	CTTGTTTAGAGCTCCATCAA	AGG
sgRNA CD48	Chr.1: 160685159-160685181	Forward	GTACATATGACCGTGGTCTC	CGG
sgRNA CD111	Chr.11:119678549 - 119678571	Forward	AATTCCACACGCTCGCGGTA	GGG

3.3 GFP mRNA electroporation in AML cell lines

AML cell lines were cultured in specific growth medium, harvested by centrifugation, and the supernatant was carefully removed. Cells were resuspended in Opti-MEM medium and centrifuged at 300 × g for 5 minutes. The 24-well plate was prepared by adding 500 μL of specific pre-warmed medium to each well and incubated at 37°C until use. For electroporation, 1×10^6 cells were resuspended in 20 μL of Opti-MEM and transferred to a 2 mm electroporation cuvette. 2 μg of mRNA was added directly to the cell suspension in the cuvette and gently mixed. Electroporation was performed using a square wave pulse under various parameter settings. Following electroporation, the cells were transferred to the pre-warmed wells of the 24-well plate and kept in the 37°C incubator. 24 hours after electroporation, flow cytometry was performed to detect electroporation efficiency.

3.4 CRISPR-Cas9-mediated electroporation in AML cell lines

AML cells were cultured in growth medium, harvested by centrifugation, and the spent medium was discarded. 500 μL of specific growth medium was added per well in a 24-well plate and maintained at 37 °C. Cells were resuspended in 1 mL of Opti-MEM medium in a 1.5 mL microcentrifuge tube and then centrifuged at 300 × g for 5 minutes. The supernatant was carefully removed. The cell pellet was again resuspended in Opti-MEM to a final concentration of 2×10^5 cells per 10 μL. Single guide RNA (sgRNA) and Cas9 protein were mixed at different ratios in RNase-free water to form a ribonucleoprotein (RNP) complex, in a volume of 5 μL, and incubated at room temperature for 10 minutes. Then, 10 μL of the cell suspension was mixed with 5 μL of the sgRNA-Cas9 RNP complex and incubated at room temperature for an additional 10 minutes. The 15 μL mixture was transferred into a 2 mm electroporation cuvette and electroporated using a previously optimized square wave condition. This procedure was described as Day 1. After electroporation, the cells were transferred to the pre-warmed 24-well plate and cultured at 32°C. On Day 2, the cells were moved to a 37°C incubator. On Day 5, we harvested the cells and used flow cytometry to assess electroporation efficiency.

3.5 Flow cytometry staining

FACS buffer was prepared by removing 15.7 mL from a 500 mL phosphate-buffered saline (PBS). To the remaining PBS, 10 mL fetal bovine serum (FBS), 4.5 mL 10% sodium azide (NaN_3), and 1.2 mL of 0.5 M EDTA were added and mixed before use. After cell counting, 4×10^5 cells were transferred into a flow cytometry tube. The cells were washed with 2 mL FACS buffer and centrifuged at 500 × g for 5 minutes at room temperature. After discarding the supernatant, 5 µL of FcR blocking reagent was added to the cells and incubated for 5 minutes. Bench lights were turned off. 0.1 µL live/dead viability dye was added to cells, mixed with a vortex, and left in the dark for 15 minutes. After incubation, cells were washed with 2 mL FACS buffer, centrifuged at 500 × g for 5 minutes, and the supernatant was discarded. Cells were then stained with the appropriate antibody, mixed with a vortex, and incubated for 30 minutes at room temperature in the dark. After staining, cells were washed again with 2 mL FACS buffer, centrifuged at 500 × g for 5 minutes at room temperature, and the supernatant was discarded. The stained samples were ready for flow cytometric analysis.

3.6 Flow cytometry analysis

Flow cytometric analysis was performed using a Fortessa flow cytometer (BD Biosciences). Flow cytometric sorting was performed using a FACSAria IIIu flow cytometer (BD Biosciences). Cell viability was evaluated by staining the samples with Zombie APC-Cy7 (BioLegend), which served as the live/dead marker. GFP expression was detected via the FITC channel. For surface marker analysis, antibodies were all obtained from Biolegend. Data acquisition was carried out with FACS Diva software version 8 (BD Biosciences) and analyzed using FlowJo X software (Version 10.0.7, BD Life Sciences, FlowJo, LLC, Ashland, OR, USA).

Table 3. Antibodies

Antibody	Cat #
APC anti-human CD155 (PVR) Antibody	337618
PE anti-human CD112 (Nectin-2) Antibody	337410
PE anti-human CD39 Antibody	328208

PE/Cyanine7 anti-human CD39 Antibody	328212
FITC anti-human CD47 Antibody	323106
FITC anti-human CD48 Antibody	336706
PE anti-human CD111 (Nectin-1) Antibody	340404
PE Mouse IgG1, κ Isotype Ctrl (FC) Antibody	400114
FITC Mouse IgG1, κ Isotype Ctrl (FC) Antibody	400110
APC Mouse IgG1, κ Isotype Ctrl (FC) Antibody	400122
PE/Cyanine7 Mouse IgG1, κ Isotype Ctrl Antibody	400126

3.7 Genomic DNA extraction

Genomic DNA was isolated from 5×10^5 cells using a peqGOLD Blood & Tissue DNA Mini Kit according to the manufacturer's protocol. Cells were pelleted by centrifugation at 1800 rpm for 5 minutes, washed with cold PBS, and resuspended in 200 µl of cold PBS. Proteinase K (25 µL) was added, and the suspension was incubated on a mixer at 300 rpm for 45 minutes to ensure complete lysis. 20 µL of RNase A (20 mg/mL) was added, and the mixture was incubated at room temperature for 2 minutes and then 10 minutes at 70 °C. After adding 220 µl ethanol, the sample was put onto the peqGOLD DNA Mini column, followed by washes with HBC Buffer and DNA Wash buffer. DNA was finally eluted with pre-warmed Elution Buffer (70 °C) and stored at -20 °C.

3.8 CRISPR-Cas9 on-target and off-target analysis

The CD48 gRNA (GTACATATGACCGTGGTCTC, PAM: CGG) was first located in the UCSC Genome Browser (https://genome.ucsc.edu/), and the genomic region including ±300 bp around the target site (9.1 Supplementary materials) was extracted for analysis. Potential off target sites were predicted by using CRISPOR (https://crispor.gi.ucsc.edu/crispor.py). On-target and selected off-target validation was performed by Patrick Blümke and his team of the High-Throughput Sequencing Technology Platform at Leibniz LIV, Hamburg, Germany. For this purpose, the human reference genome (GRCh38) was masked 500 bp upstream and downstream of the target

regions using BEDTools (Quinlan and Hall, 2010). Paired-end reads were aligned to the masked genome using the bwa mem algorithm (Li and Durbin, 2010). Aligned reads were sorted and indexed with SAMtools (Danecek et al., 2021). Reads containing deletion ("D") operations in their CIGAR strings were counted to quantify deletions within the targeted regions. Base-wise read depth, with and without deletion-containing reads, was calculated using the SAMtools depth command.

3.9 Proliferation assay

The proliferation assay was performed using the cell lines OCI-AML5 wild type (WT), single knockout CD39 (SKO CD39), double knockout PVR and PVRL2 (DKO PVR/PVRL2), and triple knockout CD39, PVR and PVRL2 (TKO CD39/PVR/PVRL2).

Day 1 (Seeding)

The cells were placed into a 50 mL tube and were mixed well before counting. Each cell line was counted at least three times by using the Beckman Coulter Vi-CELL XR cell counter. The average of the three cell counts was then used for calculating the number of seeded cells. Then each well of the 24-well plate received 1 mL of the cell suspension with 150,000 cells. The plate was kept in the incubator.

Day 4 (First Counting)

Each well was mixed by pipetting up and down several times, and 500 µL was taken for counting with the cell counter. After that, 100 µL from the remaining suspension was transferred into a new 24-well plate and mixed with 900 µL of fresh medium. The plate was returned to the incubator.

Day 8 (Second Counting)

Each well was mixed by pipetting several times, and 500 µL was taken for the final cell count.

3.10 Immune cell-mediated cytotoxicity assay

1. Isolation of PBMC and activation (Day 1)

Peripheral blood mononuclear cells (PBMCs) were obtained from healthy donors' whole blood provided by the blood bank using the Ficoll density gradient centrifugation. The blood was mixed with PBS and then carefully layered on top of the Ficoll solution. After centrifugation at 1400 × g for 30 minutes at room temperature, the white layer containing the mononuclear cells was carefully collected. The cells were washed with PBS and were ready for the following experiments. For stimulation, PBMCs were seeded in a 96-well plate. For the experimental group, Dynabeads were added at the calculated T-cell activator ratio, while the control wells received PBMCs but no beads. The plate was incubated at 37°C for 24 hours.

2. Seeding AML Cells (Day 2)

The AML cells were stained with a cell tracker green dye (CT Green) by incubation in serum-free medium for 20 minutes at 37°C in the dark. After staining and washing, the labeled AML cells were resuspended in culture medium and counted. The AML cells were then added to the PBMC-containing wells at a specific Effector-to-Target (E: T=5:1) ratio. The co-culture plate was put to the 37°C incubator for 24 hours.

3. Staining and flow cytometric analysis (Day 3)

After the co-culture period, cells from each well were transferred to 1.5 ml microcentrifuge tubes. The tubes were placed on a magnet for removing the Dynabeads, and the cell suspension was transferred to FACS tubes. The cells were washed and then treated with 7-Aminoactinomycin D (7-AAD) to label dead cells.

3.11 Statistical analysis

All data were analyzed using GraphPad Prism 7 software (GraphPad Software, Inc., San Diego, CA, USA). One-way ANOVA with Dunnett's multiple comparisons test, one-way ANOVA with Tukey's multiple comparisons analysis, two-way ANOVA with Dunnett's multiple comparisons analysis and two-way ANOVA with Tukey's multiple comparisons test were used. The FlowJo X software (Version 10.0.7, BD Life Sciences, FlowJo, LLC, Ashland, OR, USA) was used for the analysis of flow cytometry data.

3.12 Ethics statement

This study was approved by the Ethics Committee of the Hamburg Medical Association (Ethik-Kommission der Ärztekammer Hamburg, approval number PV3469). A copy of the ethics approval document is show in supplementary material 9.2.

4 Results

4.1 Generation of stable cell lines via flow cytometric sorting

After successfully delivering GFP into the AML cell lines by electroporation, CRISPR-Cas9-mediated electroporation was performed to knock out PVRL2, PVR, and CD47. In the beginning, a ratio of 7.5 pmol Cas9 with 7.5 pmol sgRNA was used. PVRL2, PVR and CD47 were expressed at nearly 100% in the wild type AML cell lines. Although the knockout experiments were successful, the efficiency of protein knockout was very low (Table 4). Taking CD47 as an example, Figure 1 shows that in the first flow cytometry analysis after electroporation, a distinct cell cluster appeared, indicating that 8.3% of the cells were successfully knocked out. After three rounds of flow cytometry sorting, a stable CD47-knockout MOLM13 cell line was obtained.

Following CRISPR-Cas9-mediated electroporation, cells were examined by flow cytometry on day 5 to confirm partial knockout of the target protein. After two or more sorting rounds, cells were analyzed again to verify that all cells lacked expression of the target protein. After 2-3 weeks of continuous culture, we confirmed the knockout was stable before freezing the cells.

For CD39, this protein exhibits a unique characteristic compared to other targets: it is not fully expressed in leukemia cell lines such as OCI-AML5. Additionally, possibly due to its association with cellular energy metabolism, stable CD39 knockout cell lines were only obtained after the 13th round of flow cytometric sorting. The data in Table 5 indicate that, although the CD39-negative cells reached a low expression level of 1.97% after the sixth round of flow cytometric sorting, subsequent measurements over the following two weeks showed an increase in CD39 expression to 5.56% and 13.9%. Following the establishment of the cell line after 13 rounds of sorting, flow cytometry analyses were performed during the first, second, and third week (Figure 2). After confirming negative results at each time point, the knockout cell lines were cryopreserved.

PVR and PVRL2 are expressed at nearly 100% in OCI-AML5, TF-1, KG-1, UKE-1 and MOLM13 cells, so fewer rounds of sorting are needed to obtain the negative cells. CD47 is also expressed at 100% in MOLM13 and TF-1 cells. Therefore, for these target proteins, sorting the negative populations two to four times is sufficient to establish stable knockout cell lines. The following table lists the knockout cell lines that have been

established so far, along with the number of flow cytometry sorting rounds performed for each line (Table 6).

Table 4.

CRISPR-Cas9-mediated knockout	Cell line	Percentage of Protein Knockout in AML Cells (%)
PVRL2	MOLM13	0.70%
	TF-1	2.50%
	OCI-AML5	0.60%
	KG-1	0.40%
	UKE-1	4.8%
PVR	MOLM13	2.80%
	TF-1	0.80%
CD47	MOLM13	8.3%

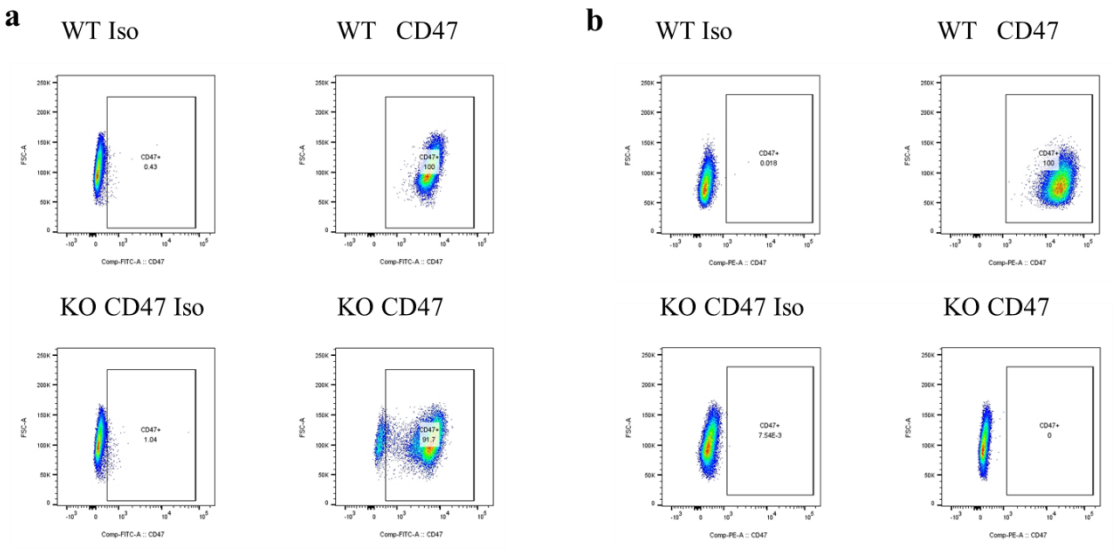

Figure 1. Flow cytometry analysis of CD47 knockout efficiency in MOLM13 cells.

(a) First flow cytometry analysis after electroporation showing initial CD47 knockout efficiency in Molm13 cell line. (b) After three rounds of sorting, we analyzed the cells again by flow cytometry. The results showed that a stable CD47-knockout population had been successfully obtained.

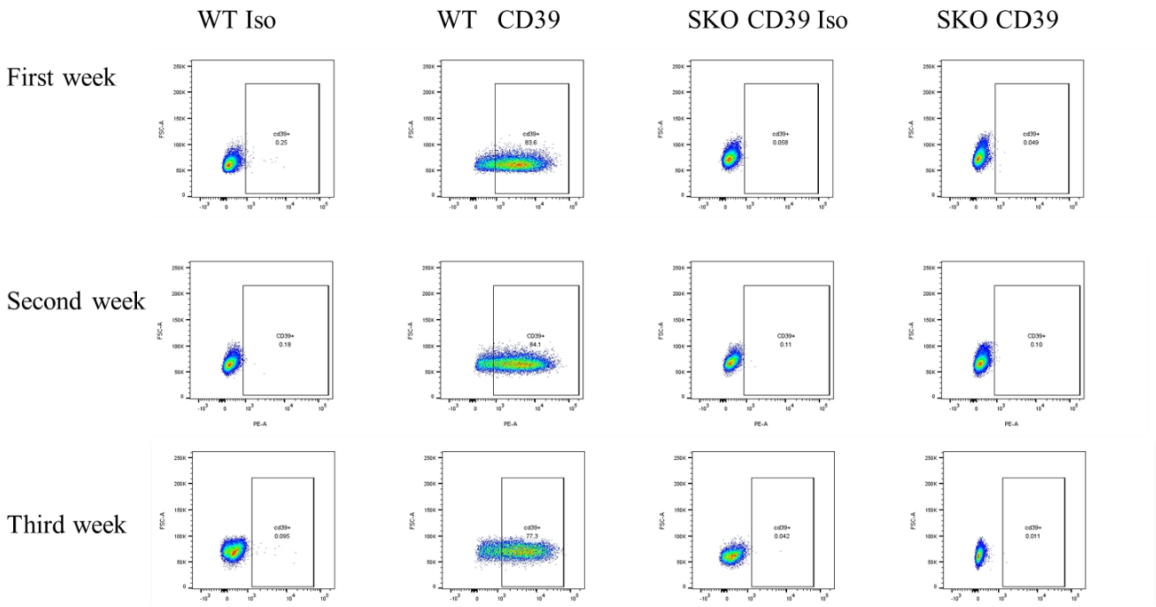

Figure 2. Weekly flow cytometry analysis of CD39 expression after CRISPR-Cas9 editing in OCI-AML5 cells.

OCI-AML5 cells were electroporated with CRISPR-Cas9 to knock out CD39 and then sorted 13 times by flow cytometry. After sorting, the cells were cultured for the following three weeks, and CD39 expression was checked once per week. The plots labeled WT show the OCI-AML5 wild type cells, which normally express CD39. The Iso plots represent the isotype negative control used to indicate background staining. Across all three weeks, the edited cells showed no detectable CD39, suggesting a stable knockout.

Based on the results above, we realized that using the current experimental procedures, the efficiency of knocking out the target proteins was very low. We speculated that optimizing the experimental steps might improve the knockout efficiency, so we carried out optimization experiments combining electroporation with CRISPR-Cas9 in the next.

Table 5. The expression of CD39 in OCI-AML5 wild type and CD39 knockout cells

A. CD39 expression after different rounds of cell sorting

Round of sort for CD39 varients	Percentage of CD39 expression in CD39 KO cells (%)	Percentage of CD39 expression in wild type cells (%)
1	2.17%	74.7%
3	4.48%	87.3%
5	2.64%	94.8%
6	1.97%	59.5%
7	0.43%	59.5%
9	0.18%	71.1%
10	0.38%	69.3%
13	0.00%	83.6%
13	0.00%	84.1%
13	0.00%	77.3%

B. CD39 re-expression after sorting.

Round of sort for CD39 varients	Weeks after sorting	Percentage of CD39 expression in CD39 KO cells (%)
6	1	1.97%
6	2	5.56%
6	3	13.9%
9	1	0.18%
9	2	1.88%

Table 6. Summary of Generated Knockout Cell Lines.

CRISPR-Cas9-mediated knockout	Cell line	Rounds of sorting to reach complete knockout
CD47	MOLM13	3
	TF-1	3
PVRL2	MOLM13	2
	TF-1	3
	OCI-AML5	4
	KG-1	2
	UKE-1	2
PVRL2 + PVR	MOLM13	3
	TF-1	3
	OCI-AML5	2
PVRL2 + PVR+CD47	MOLM13	3
	TF-1	3
CD39	OCI-AML5	13
PVRL2 + PVR+CD39	OCI-AML5	12

4.2 Workflow for electroporation optimization and CRISPR-Cas9 application in AML Cells

As shown in Figure 3, the optimization of electroporation was conducted in two parts. In the first part, six different electroporation conditions (100 V 5 ms, 100 V 10 ms, 150 V 5 ms, 150 V 10 ms, 200 V 5 ms, and 200 V 10 ms) were tested on three different AML cell lines (MOLM-13, OCI-AML5, and TF-1). In the second part, electroporation of different CRISPR-Cas9 RNPs into AML cells was performed to further optimize RNP delivery and editing efficiency.

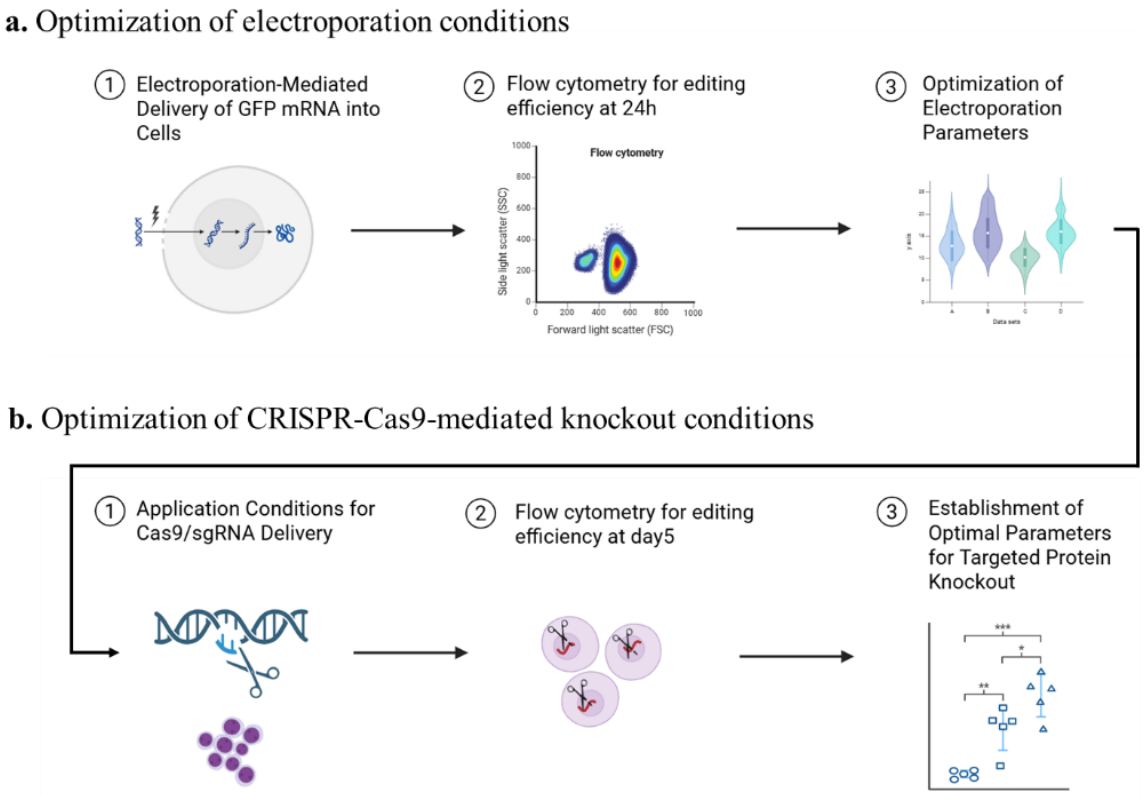

Figure 3. Workflow for optimization of electroporation parameters and application to CRISPR-Cas9-mediated protein knockout. Created with BioRender.com.

(a) 1. GFP mRNA was delivered into three different AML cell lines via electroporation. 2. At 24 hours, flow cytometry was used to assess transfection efficiency and viability. 3. Based on the flow cytometry data, electroporation conditions were optimized to identify the most efficient and least cytotoxic parameters. (b) 1. The optimal electroporation parameter was then applied to deliver Cas9 protein complexed with synthetic sgRNAs targeting CD48 or CD111. 2. Editing efficiency was evaluated by flow cytometry at day 5 post-electroporation. 3. Different molar ratios of Cas9 with sgRNA

were tested, and editing efficiency was quantified to establish the optimal conditions for targeted protein knockout.

4.3 Impact of different electroporation conditions on cell viability

We performed electroporation with GFP mRNA on Molm13, OCI-AML5, and TF-1 cell lines at room temperature. For each electroporation, 1 million cells were resuspended in 20 µL of Opti-MEM buffer, mixed with 2 µg of GFP mRNA, and transferred into a 2 mm cuvette. Six electroporation conditions were tested: 100 V 5 ms, 100 V 10 ms, 150 V 5 ms, 150 V 10 ms, 200 V 5 ms, and 200 V 10 ms. All electroporation conditions used a square wave with a single pulse. Cell viability was assessed by flow cytometry 24 h after electroporation. One-way ANOVA showed significant differences in cell viability among electroporation conditions in MOLM13, OCI-AML5, and TF-1 cell lines (all $P< 0.0001$). Under the 150 V 5 ms condition, cell viability was still high, with mean viabilities of 91.5% for MOLM13, 95.7% for OCI-AML5, and 94.7% for TF-1 cells. No significant reduction in viability was observed under these conditions, including 100 V 5 ms, 100 V 10 ms, and 150 V 5 ms, compared with unelectroporated control cells. In contrast, cell viability declined markedly when cells were electroporated at 150 V for 10 ms, and this reduction became stronger at higher voltage settings. Electroporation at 150 V 10 ms and at both 200 V conditions resulted in statistically significant decreases in viability across all three cell lines compared with control samples ($P< 0.05$ to $P < 0.0001$) (Figure 4).

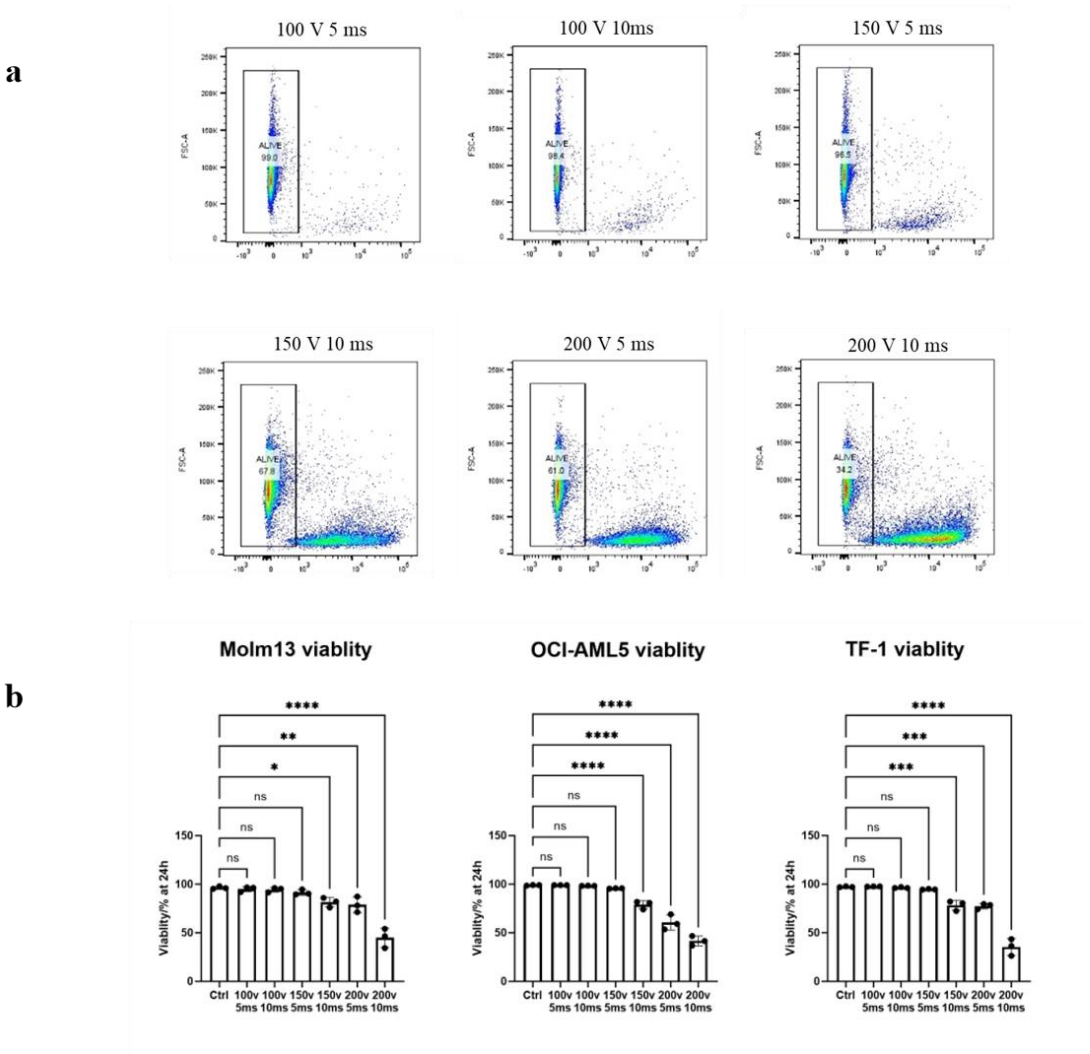

Figure 4. Electroporation based viability changes in MOLM13, OCI-AML5, and TF-1 cell lines under different electroporation conditions.

(a) Representative flow cytometry plots of OCI-AML5 cells after electroporation with GFP mRNA showing the proportion of viable cells under six electroporation conditions (100 V 5 ms, 100 V 10 ms, 150 V 5 ms, 150 V 10 ms, 200 V 5 ms, 200 V 10 ms). (b) Quantification of cell viability from three independent experiments. MOLM13, OCI-AML5, and TF-1 cells were electroporated with GFP mRNA under the six voltage and pulse duration settings as indicated above. Viability was assessed 24 h post electroporation using Zombie viability dye and flow cytometry. The percentage of viable (Zombie-negative) cells was quantified using FlowJo. Statistical evaluation was performed with GraphPad Prism, and data are presented as mean ± SD of three independent experiments. Statistical analysis was performed using one-way ANOVA with Dunnett's multiple comparisons test. ns, not significant; *p < 0.05; **p < 0.01; ***p < 0.001; ****p < 0.0001.

4.4 Effects of different electroporation conditions on cell transfection efficiency

To determine the optimal electroporation condition for GFP mRNA delivery, we evaluated transfection efficiency across six different electroporation settings in MOLM13, OCI-AML5, and TF-1 cell lines. 24 hours after electroporation, GFP expression in the cells was evaluated using flow cytometry. And the measurements were analyzed with FlowJo. The efficiency of transfection was evaluated based on the proportion of cells expressing GFP. As shown in Figure 5b, electroporation at 150 V for 5 ms consistently produced the highest average GFP expression in all three cell lines (MOLM13: 81%; OCI-AML5: 81.2%; TF-1: 76.7%). In individual experiments, higher GFP levels were occasionally observed (MOLM13: 89.5%; OCI-AML5: 85.6%; TF-1: 85.2%). Statistical analysis using one-way ANOVA showed that GFP expression varied significantly among electroporation conditions in MOLM13 ($P = 0.001$) and OCI-AML5 ($P < 0.0001$), while no significant differences were observed in TF-1 ($P = 0.11$). Tukey's multiple comparison analysis showed that, in MOLM13, 150 V 5 ms was significantly higher than 100 V 5 ms ($P = 0.0012$), while no significant difference was observed compared with 100 V 10 ms or any of the higher voltage or longer pulse conditions. In OCI-AML5, GFP levels at 150 V 5 ms were significantly greater than those at the lower voltage settings (100 V 5 ms and 100 V 10 ms) and the condition (200 V 10 ms), whereas differences with 150 V 10 ms and 200 V 5 ms were not statistically significant. In TF-1 cells, no significant differences were detected among the different groups, although the highest average GFP expression was observed at 150 V 5 ms. In total, these findings suggest that 150 V 5 ms generally produced the highest average GFP expression among the conditions tested (Figure 5).

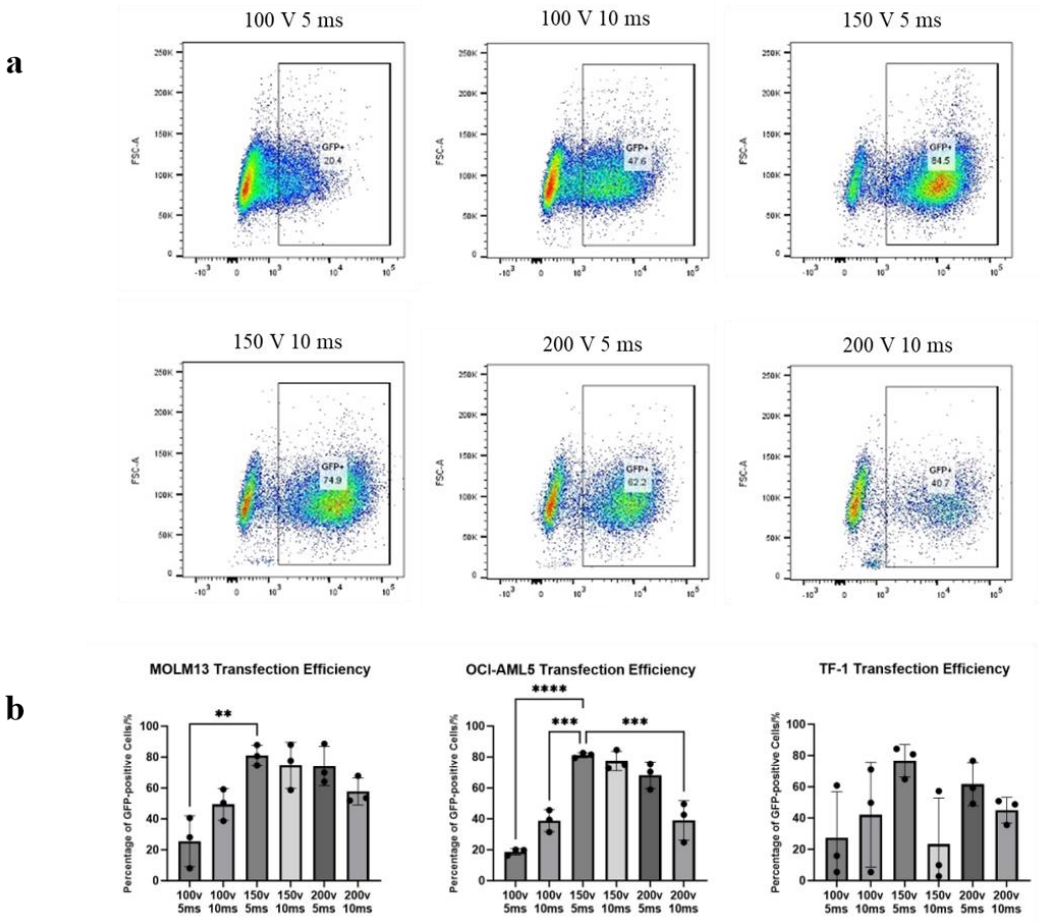

Figure 5. Transfection efficiency of GFP mRNA in acute leukemia cell lines under different electroporation conditions.

(a) Representative flow cytometry plots of OCI-AML5 cells after electroporation with GFP mRNA showing the expression of GFP under six electroporation conditions (100 V 5 ms, 100 V 10 ms, 150 V 5 ms, 150 V 10 ms, 200 V 5 ms, 200 V 10 ms). (b) MOLM13, OCI-AML5, and TF-1 cells were electroporated with GFP mRNA using six different voltage and pulse duration settings. GFP expression was assessed by flow cytometry 24 hours after electroporation. Data were analyzed using FlowJo, and the efficiency of transfection was evaluated based on the proportion of cells expressing GFP. Statistical analysis was performed using one-way ANOVA with Tukey's multiple comparison analysis. Data from three independent experiments are presented as mean ± SD. In MOLM13, GFP expression at 150 V 5 ms was significantly higher than at 100 V 5 ms ($P = 0.0012$), but no significant differences were observed compared with any other conditions. In OCI-AML5, 150 V 5 ms produced significantly greater GFP expression than 100 V 5 ms ($P < 0.0001$), 100 V 10 ms ($P = 0.0002$), and 200 V 10 ms ($P = 0.0002$), whereas differences with other conditions were not statistically significant. In TF-1 cells,

no significant differences were detected among the conditions, although the highest average GFP expression was observed at 150 V 5 ms. ns, not significant; **p < 0.01; ***p < 0.001; ****p < 0.0001.

4.5 Electroporation mediated CRISPR-Cas9 genome editing in acute myeloid leukemia cell lines

Using the optimized electroporation condition of 150 V for 5 ms, as detailed above, we attempted to knock out two proteins, CD48 and CD111, in acute myeloid leukemia cell lines. Before performing the knockout experiments, we assessed the expression levels of CD111 and CD48 in the AML cell lines by flow cytometry (Figure 6). CD111 was highly expressed in MOLM-13 and OCI-AML5 cells, with expression levels of 88.6% and 97.8%, respectively. CD48 expression in OCI-AML5 cells reached 98.6%.

a. The expression of CD111 in MOLM13

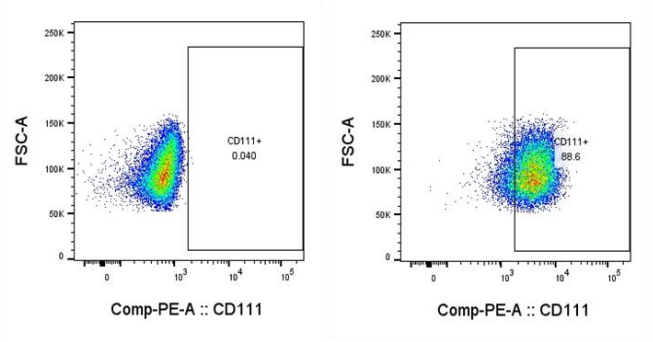

b. The expression of CD111 in OCI-AML5

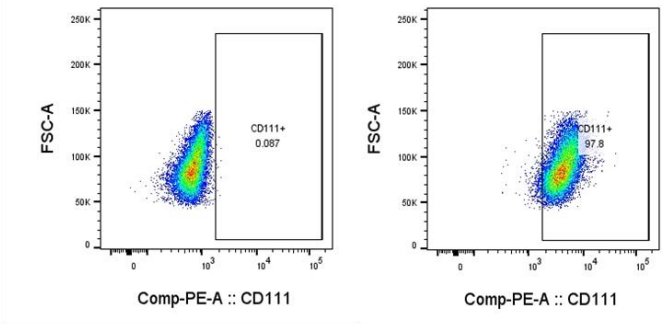

c. The expression of CD48 in OCI-AML5

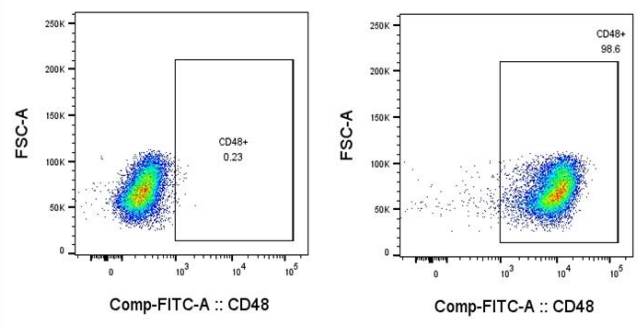

Figure 6. Flow cytometry analysis of CD111 and CD48 expression in AML cell lines.

(a) CD111 expression in MOLM-13 cells, showing 88.6% $CD111^+$. (b) CD111 expression in OCI-AML5 cells, showing 97.8% $CD111^+$. (c) CD48 expression in OCI-AML5 cells, showing 98.6% $CD48^+$.

We performed CD111 and CD48 knockouts in OCI-AML5 cells, and the CD111 knockout in MOLM13 cells. We tested three different concentration combinations: 7.5 pmol Cas9 with 7.5 pmol sgRNA, 37.5 pmol Cas9 with 37.5 pmol sgRNA, and 37.5 pmol Cas9 with 75 pmol sgRNA. As shown in figure 7, in OCI-AML5 and MOLM13 cell lines, depletion of CD111 protein was unsuccessful at the lowest RNP dose. When the intermediate dose was applied, protein depletion remained inefficient, achieving only around 6% even in successful attempts. In contrast, the highest dose led to an increase, with mean depletion reaching approximately 46.7% and 31.4%, respectively. Statistical analysis using one-way ANOVA showed that a significant difference among treatment groups for CD111 knockout in OCI-AML5 cells ($P = 0.0028$). There was no statistical significance ($P = 0.0914$) for CD111 knockout in MOLM13 cells. For CD48 knockout in OCI-AML5 cells, all three RNP combinations were able to achieve successful protein depletion and the knockout efficiency increased with higher Cas9 and sgRNA concentrations. In addition, the highest knockout efficiency was observed at the highest dose, reaching up to the average of 62.4%. One-way ANOVA showed a significant difference of RNP concentration on CD48 knockout efficiency ($P = 0.0056$), and Tukey's multiple comparison analysis confirmed that the highest dose showed significantly difference from the lower dose conditions. In all experiments, higher concentrations of Cas9 and sgRNA resulted in increased knockout efficiency, with the combination of 37.5 pmol Cas9 and 75 pmol sgRNA achieving the highest knockout in each case (Figure 7).

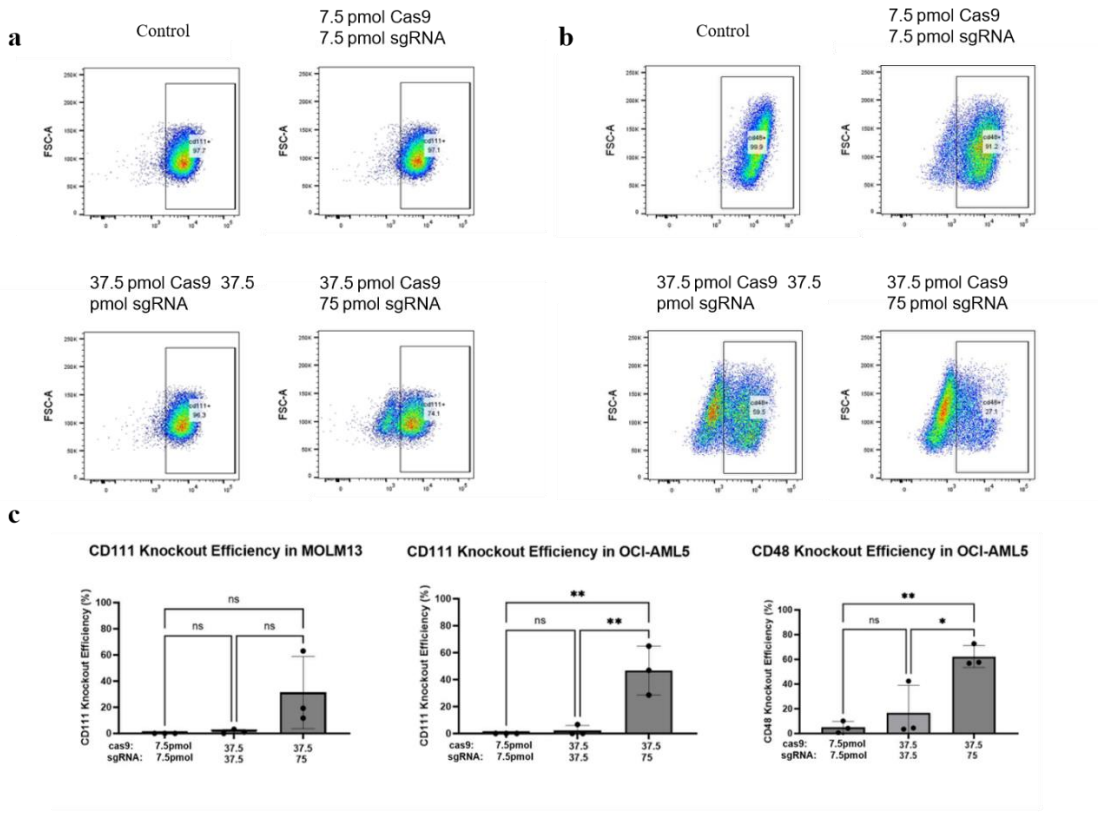

Figure 7. Knockout efficiency of CD111 and CD48 in MOLM13 and OCI-AML5 cell lines.

(a) Representative flow cytometry plots showing CD111 knockout in MOLM13 cells after electroporation with different RNP. (b) Representative flow cytometry plots showing CD48 knockout in OCI-AML5 cells after electroporation with different RNP. (c) Quantification of CD111 knockout efficiency in MOLM13 (left) and OCI-AML5 (middle), and CD48 knockout efficiency in OCI-AML5 (right). Cells were electroporated with 7.5 pmol Cas9 + 7.5 pmol sgRNA, 37.5 pmol Cas9 + 37.5 pmol sgRNA, or 37.5 pmol Cas9 + 75 pmol sgRNA. Each condition was repeated in three independent experiments. The expression of the target protein in wild type control groups was normalized to 1 in each experiment due to variations in baseline expression. For each condition, the average value from two electroporations was calculated and then normalized to the corresponding control. Statistical analysis was performed using one-way ANOVA with Tukey's multiple comparison analysis. Data are presented as mean ± SD from three independent experiments. ns, not significant; *$p < 0.05$; **$p < 0.01$.

4.6 On-target editing of CD39 and CD48 and off-target analysis of CD48 in CRISPR-Cas9–mediated editing

CD48 knockout was performed using three different RNP doses with CRISPR-Cas9 technology. They were low (7.5 pmol Cas9 + 7.5 pmol sgRNA), medium (37.5 pmol Cas9 + 37.5 pmol sgRNA), and high (37.5 pmol Cas9 + 75 pmol sgRNA). At first, we evaluated the CD48 knockout rates under different RNP concentrations by flow cytometry, which were 1%, 1.7%, 25.6%, 25.6%, 55.6%, and 46.4% across six samples. Then we assessed their editing efficiency by sequencing, which showed 9.23%, 9.66%, 24.56%, 24.16%, 35.39%, and 29.89% of on-target editing. Higher RNP concentrations led to higher knockout rates. No editing was detected in the wild type control cells. In the on-target sequencing analysis of CD39, we also obtained ideal results. Two samples were analyzed: one wild type sample and one CD39 complete knockout sample validated by flow cytometry. The sequencing results of on-target knockout efficiencies were 0.01% and 96.64%, respectively. Editing efficiency for each sample was calculated as the percentage of reads with deletions relative to total reads. The sequencing results all matched the flow cytometry data, showing that the CRISPR-Cas9 knockout was evident at both the protein and DNA levels.

We evaluated two predicted off-target sites, ASXL3 and RAB4B, after knocking out CD48 with CRISPR-Cas9 in OCI-AML5 cells. The editing at these sites was all very low in each treatment group and similar to the wild type samples, suggesting that off-target effects were minimal. Although CRISPOR (https://crispor.gi.ucsc.edu/crispor.py) predicted five possible off-target sites, we only tested ASXL3 and RAB4B in our experiment. As both on-target and off-target analysis were performed once, no statistical analysis was performed (Figure 8).

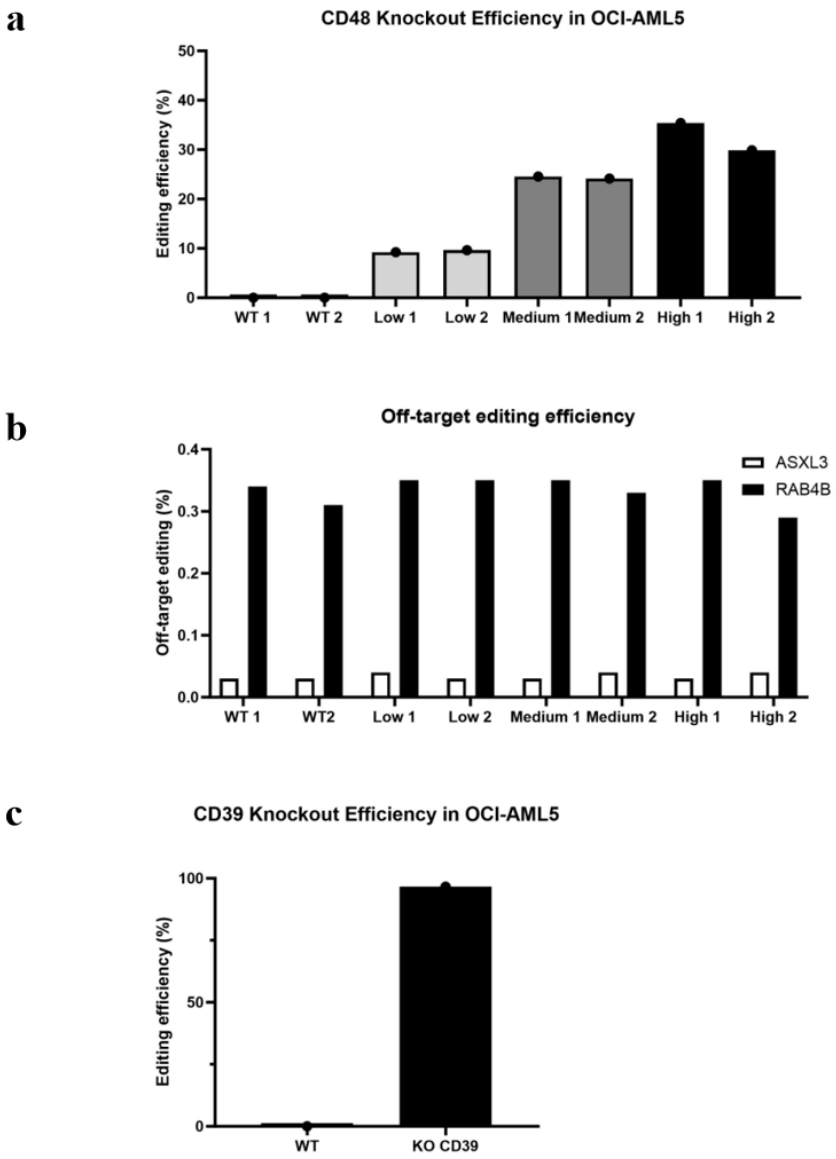

Figure 8. On-target editing efficiency of CD48 and CD39 and off-target editing efficiency of CD48, measured by sequencing, in OCI-AML5 cells after CRISPR-Cas9–mediated knockout of either CD48 or CD39 at varying RNP concentrations. (a) Each bar represents the on-target editing efficiency of CD48 in OCI-AML5 cells for each sample, calculated as the percentage of reads with deletions relative to total reads. Low, medium, and high concentrations correspond to 7.5 pmol Cas9 + 7.5 pmol sgRNA, 37.5 pmol Cas9 + 37.5 pmol sgRNA, and 37.5 pmol Cas9 + 75 pmol sgRNA, respectively. WT represents the wild type control. (b) Each bar represents the off-target editing efficiency of CD48 in OCI-AML5 cells for each sample. (c) Each bar represents the on-target editing efficiency of CD39 in OCI-AML5 cells for each sample. All on-target and off-target experiments were performed once without statistical analysis.

4.7 Proliferation of OCI-AML5 WT and CD39/PVR/PVRL2 knock out variants

We evaluated the proliferation of OCI-AML5 cells with different gene knockouts at day 4 and day 8, including OCI-AML5 WT, single knockout CD39 (SKO CD39), double knockout PVR and PVRL2 (DKO PVR/PVRL2), and triple knockout CD39, PVR and PVRL2 (TKO CD39/PVR/PVRL2). Cell numbers were counted by using the Beckman Coulter Vi-CELL XR cell counter. Statistical analysis was performed by using two-way ANOVA. The result showed no significant interaction between genotype and time, and no significant differences between genotypes in cell proliferation. These findings indicate that deletion of CD39, PVR, and PVRL2, alone or in combination, does not markedly affect the proliferation of OCI-AML5 cells (Figure 9).

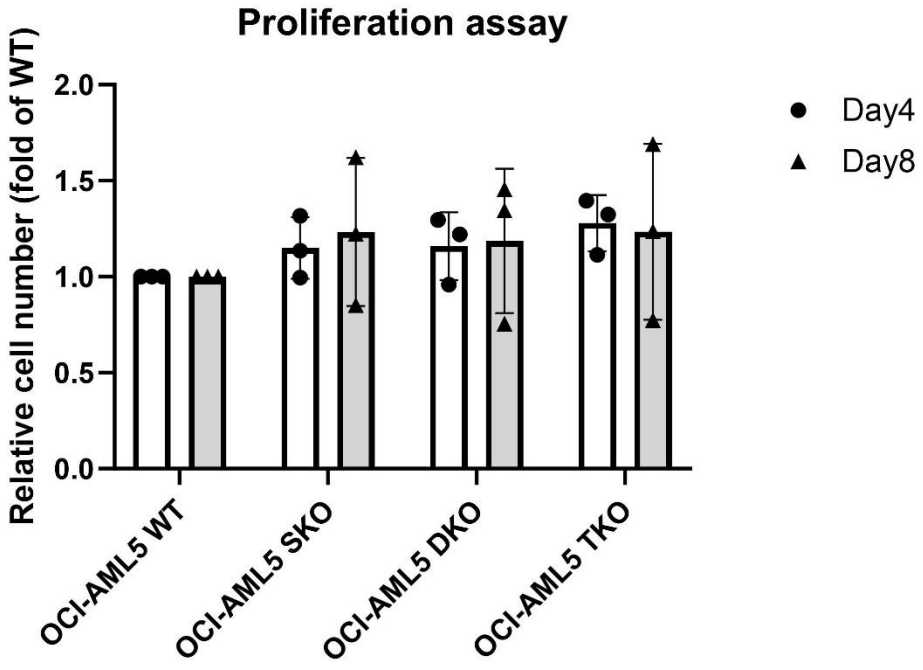

Figure 9. Proliferation analysis of OCI-AML5 cells with different gene knockouts.

Proliferation of OCI-AML5 WT, single knockout CD39 (SKO CD39), double knockout PVR and PVRL2 (DKO PVR/PVRL2), and triple knockout CD39, PVR and PVRL2 (TKO CD39/PVR/PVRL2) cells were measured on day 4 and day 8. Cells were counted by using the Beckman Coulter Vi-CELL XR cell counter. Data were analyzed by two-way ANOVA with Tukey's multiple comparisons test. No statistically significant differences were detected between groups. Data are presented as mean ± SD from three independent experiments.

4.8 Immune cell-mediated cytotoxicity assay of OCI-AML5 WT and CD39/PVR/PVRL2 knockout variants

We attempted to compare the tumor-killing capabilities of the following four cell lines, including OCI-AML5 WT, single knockout CD39 (SKO CD39), double knockout PVR and PVRL2 (DKO PVR/PVRL2), and triple knockout CD39, PVR and PVRL2 (TKO CD39/PVR/PVRL2). Healthy donor PBMCs were first co-cultured with Dynabeads carrying CD3/CD28. Then, the PBMCs were co-cultured with the different AML cell lines. In each experiment, each cell line was divided into two groups: one group was co-cultured with stimulated PBMCs, and the other group was co-cultured with unstimulated PBMCs. Two-way ANOVA analysis showed a significant effect of cell line ($P= 0.0053$) and PBMC stimulation ($P= 0.0199$), but no significant interaction between cell line and stimulation ($P = 0.7175$). In the absence of stimulated PBMCs, an average of 18.8% of WT AML cells were killed, whereas all the other knockout lines showed lower values. SKO CD39 cells were 12.0%, DKO PVR/PVRL2 cells were 14.7%, and TKO CD39/PVR/PVRL2 cells dropped to 6.0%. Dunnett's multiple comparisons test indicated that none of the knockout groups were significantly different from WT under unstimulated conditions, although TKO cells showed a trend toward lower killing ($P = 0.0952$). A similar trend was observed with stimulated PBMCs. When PBMCs were stimulated with CD3/CD28 Dynabeads, AML cell killing increased in all groups. WT cells were killed most efficiently, with 30.2%. The knockout cells were still killed less: 19.8% of SKO CD39, 20.2% of DKO PVR/PVRL2, and 9.5% of TKO CD39/PVR/PVRL2 cells. Dunnett's multiple comparisons analysis showed that only TKO cells showed significantly reduced killing compared with WT ($P = 0.0041$). These findings show that deleting CD39, PVR, or PVRL2 does not increase AML cell killing. In total, these results indicate that gene deletion does not lead to a higher killing response when compared with WT cells. Instead, the killing efficiency decreases from WT to SKO, DKO, and TKO (Figure 10).

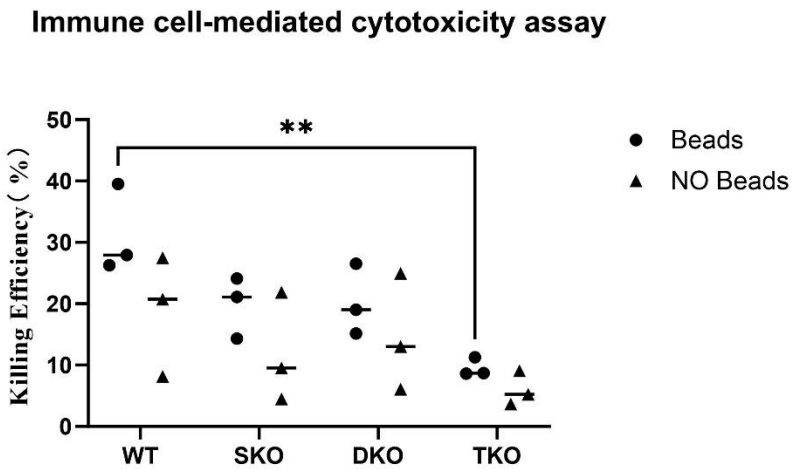

Figure 10. Comparison of immune cell-mediated cytotoxicity assay among OCI-AML5 WT cells and different gene knockouts.

The bar graph presents the killing efficiency (%) of the four different cell lines under unstimulated and beads-stimulated conditions. The cell lines are OCI-AML5 WT, single knockout CD39 (SKO CD39), double knockout PVR and PVRL2 (DKO PVR/PVRL2) and triple knockout CD39, PVR and PVRL2 (TKO CD39/PVR/PVRL2). Each bar shows the mean ± SD from three independent experiments. Statistical analysis was performed using two-way ANOVA with Dunnett's multiple comparisons analysis. TKO cells showed significantly reduced killing compared with WT under stimulated condition ($P = 0.0041$). Only statistically significant comparisons are shown. **$p < 0.01$.

5. Discussion

5.1 Methodological aspects of electroporation optimization

Electroporation is widely used as a non-viral delivery method because it is easy to operate and can transfer different biomolecules into many cells at one time. Although the methods used in cell therapy sometimes lead to low transfection efficiency and cell damage, electroporation is still considered a practical and promising approach (Potočnik et al., 2022, Kang et al., 2015). Over the past decade, the application of electroporation has greatly advanced the research and treatment of diseases (Golberg et al., 2016, Desbiolles et al., 2020). In this study, we attempted to investigate reproducible and highly efficient electroporation of AML cell lines, which is crucial for research on AML immunotherapy. To our delight, we found that the MOLM13, OCI-AML5, and TF-1 cell lines all exhibited the highest transfection efficiency and high cell viability under the condition of 150 V for 5 ms square wave pulse. MOLM13, OCI-AML5, and TF-1 cell lines are all commonly utilized in AML research to study gene regulation and signaling pathways (Wu et al., 2023, Freisleben et al., 2020, Lee et al., 2021). In our experiments, we tested electroporation with GFP mRNA in these three different cell lines and used the optimized electroporation condition for CRISPR-Cas9 mediated proteins knockout. We specially used the square-wave pulse for electroporation, as this wave form has been shown to be optimal for mammalian cell transfection (Hyder et al., 2020). Electric field strength, pulse duration and electroporation buffer are important parameters to adjust when optimizing electroporation conditions (Bajwa et al., 2023, Cemazar et al., 2002). In our study, electroporation at 150 V for 5 ms square wave pulse gave the best balance between cell survival and GFP mRNA delivery efficiency. Compared with the condition of 150 V 5 ms, when we extended the pulse time to 150 V 10ms, or increased the voltage to 200 V 5ms, the cell viability and electroporation efficiency both decreased after electroporation. Previous work by Hyder et al. showed that Opti-MEM with GlutaMax outperformed other electroporation buffers in terms of cell viability and successfully transferred genetic material. In their study, the other tested media were Gene Pulser electroporation buffer (Bio-Rad), phosphate-buffered saline (PBS), and D10 cell culture medium (Hyder et al., 2020). GlutaMax is a more stable form of L-glutamine (Devireddy et al., 2019). In our study, we used Opti-MEM® I Reduced Serum Medium containing standard L-glutamine, which was sufficient to achieve high cell viability and transfection efficiency. In addition to the choice of electroporation buffer, serum has been found to

modulate cell viability in earlier studies during electroporation without negatively affecting gene transfer (Delteil et al., 2000). In the present study, Opti-MEM without serum was used, but future work could consider the effect of serum supplementation on electroporation outcomes.

I also attempted three times to apply the same electroporation protocol to primary bone marrow mononuclear cells isolated from acute leukemia patients. However, all attempts failed to achieve detectable transfection. This suggests that the optimized parameters established for AML cell lines are not directly suitable to primary cells. This aligns with the consensus among many scientists that primary leukemia cells are difficult to transfect (Shin and Min, 2023, Terziyska et al., 2012). In future work, further optimization of the electroporation conditions will be needed in order to achieve efficient gene delivery in primary leukemia cells as well. This may include adjusting the pulse settings, modifying the buffer composition , culture medium required for cell resuscitation (Alawar et al., 2024) and the molecular format of the cargo (Pathak et al., 2023). In addition, we could also consider incorporating nucleofection in the future to optimize electroporation of primary leukemia cells. Although Schakowski et al. successfully performed nucleofection on primary cells from three AML patients, achieving transfection rates up to 75%, the cells ultimately died (Schakowski et al., 2004). Therefore, transfection methods suitable for long-term experiments with primary cells still need to be explored.

5.2 Optimization for CRISPR-Cas9 mediated electroporation

Genetic modification is an important approach to study tumor development and progression. CRISPR-Cas9 has become a powerful tool for precise genome editing (Uddin et al., 2020, Chehelgerdi et al., 2024). However, for leukemic cells, editing efficiency and cell survival are highly dependent on experimental conditions. Therefore, the aim of this study was to optimize the knockout procedure in leukemic cells. Designing guide RNAs is a key step in setting up experiments, and a variety of tools exist to predict gRNA candidates with low likelihood of off-target activity (Enssle et al., 2025). All the sgRNA and Cas9 protein we used in this study were purchased from Thermo Fisher Scientific. All sgRNAs were selected based on the top predicted on-target scores provided by the Invitrogen™ TrueGuide™ Synthetic gRNA design tool from Thermo Fisher Scientific. According to their user guide, 7.5 pmol Cas9 together with 7.5 pmol

sgRNA are recommended as the starting concentrations for use with the Neon™ Transfection System. Although we used the Bio-Rad Gene Pulser Xcell system instead of the Neon system, we still performed electroporation with the same initial concentration of RNP. Covello et al. reported that the Gene Pulser Xcell system exhibits higher efficiency than lipid-based transfection methods. While the Neon system is usually more effective for PC12 cells, the Gene Pulser Xcell system provides better cell viability and outperforms lipid-based approaches (Covello et al., 2014).

CD48 and CD111 are both cell surface proteins belonging to the immunoglobulin superfamily. It has been summarized by McArdel et al. that CD48 is upregulated in a range of hematologic malignancies (McArdel et al., 2016). Soluble CD48 was found to be increased in the serum of individuals with leukemia or lymphoma (Smith et al., 1997). Poliovirus receptor (PVR) and poliovirus receptor-related protein 2 (PVRL2) are key ligands of poliovirus receptor (PVR)-like proteins and have been identified as novel immune checkpoints (Stamm et al., 2018a, Yang et al., 2024). CD111 (PVRL1 or nectin-1) also functions as a ligand of PVR-like proteins (Wu et al., 2021). However, whether and how CD111 contributes to immune responses in cancer cells remains to be elucidated.

We found that the ratio of RNP affected knockout efficiency. For CD111, low doses did not reduce protein levels, medium doses gave only about 6% knockout at most, and the highest dose improved efficiency to around 46.7% and 31.4%. For CD48, knockouts worked at all doses, but the highest dose was needed to reach the best efficiency of 62.4%. This suggests that for different protein knockouts, their sensitivity to the lowest concentration of RNP electroporation knockdown is different. Nevertheless, when this concentration ratio of RNP was used, 37.5 pmol Cas9 and 75 pmol sgRNA achieved the highest knockout efficiency for different proteins in different cell lines. These observations are in line with Yuen et al (Yuen et al., 2017), who demonstrated that sgRNA intrinsic efficacy and high levels of Cas9 and sgRNA expression could improve target knockout efficiency. In our experiments, low RNP doses failed to achieve effective protein depletion, whereas higher doses reached the threshold necessary for substantial knockout. As different proteins have different original expression levels in cell lines, we would recommend that when you are faced with the problem of knocking out a new protein, using our recommended concentration will improve the efficiency of the experiment. Our strategy was to first confirm the successful knockout of the protein at the protein level by flow cytometry after electroporation, and then use flow cytometric

cell sorter to obtain cells with negative protein expression. The higher the knockout efficiency, the less the number of flow cytometry sorting and the time to establish a stable knockout cell line. In future, our strategy could make it easier to knock out targets like CD39 and reduce the number of sorting rounds.

For the analysis of the on-target and off-target CD48 CRISPR-Cas9-mediated editing, we found that the knockout results from flow cytometry were consistent with the on-target editing efficiencies measured by sequencing. This agreement supports the reliability of our CRISPR-Cas9 knockout strategy. The off-target editing efficiency of ASXL3 and RAB4B was similar to wild-type cells and is probably due to limitations and inaccuracies of NGS sequencing, suggesting minimal off-target effects. However, only a limited number of samples and predicted off-target sites were analyzed, which is a limitation of this study and should be addressed in future experiments.

5.3 Understanding the lack of functional effects after CD39 ko in AML cells

Based on previous experimental data and verification by flow cytometry (Figure 2, Table 5), we confirmed the successful generation of the CD39 protein knockout cell line. Furthermore, based on the findings from several studies on CD39, we speculate that CD39 knockout may inhibit tumor cell proliferation, enhance the ability of T cells to kill tumor cells, and ultimately contribute to a stronger anti-tumor effect (Sun et al., 2010, Feng et al., 2011, Liu et al., 2022a, Tsai and Stromnes, 2024, Bastid et al., 2013). However, according to our results, knocking out CD39 did not either reduce the proliferation of OCI-AML5 cells or increase tumor cell death. The enzymes CD39 and CD73 convert ATP into immunosuppressive adenosine. A2AR is a receptor for adenosine and its activation can reduce the activity of immune cells (Myojin et al., 2024, Priyadharshini and Turka, 2015). Mohammadian Gol et al. reported that knocking out A2AR had little effect on cell function. On the other hand, Brauneck et al. from our research group showed that blocking A2AR with an antagonist improved the ability of NK-92 cells to kill AML cells, especially when combined with TIGIT inhibition. These differences might be due to the different methods used, such as CRISPR knockout versus drug treatment, and the different AML cell lines. CD39 is expressed on some AML cells but is mainly expressed on immune cells in the tumor microenvironment. Therefore, knocking out CD39 in AML cell lines only affects its function in leukemia cells and has no direct influence on the conversion of ATP by surrounding immune cells expressing

CD39. Brauneck et al. reported blocking CD39 with the nanobody SB24 enhanced T cell proliferation and killing of AML cells. Although this effect was stronger in AML patients where the leukemic blasts had a high CD39 expression, one cannot directly compare the findings from the CD39 knockout approach to the nanobody blocking experiments (Mohammadian Gol et al., 2023, Brauneck et al., 2021, Brauneck et al., 2024, Weimer et al., 2022, Witt et al., 2024, Liu et al., 2023). The implication for our study is that in the future, we could also try to test different cell lines and consider using nanobodies to block CD39 expression or other approaches to inhibit CD39 expression, in order to compare the effects of various CD39 inhibition methods on anti-tumor activity.

In tumors, stressed or dying cells release ATP into the tumor microenvironment (TME). CD39 converts the ATP into AMP, and CD73 then produces adenosine from AMP. Because CD39 and CD73 are often highly expressed in tumors, adenosine accumulates to high levels, resulting in immune suppression in the TME (Xia et al., 2023, Han et al., 2022, Liu et al., 2023). Although CD39 and CD73 are the main enzymes that produce extracellular adenosine, adenosine can also be generated by other pathways. For example, CD38 and CD203a can convert NAD^+ to AMP, which CD73 then changes to adenosine. Other enzymes, like CD203a/CD203c, prostatic acid phosphatases (PAPs) and tissue-non-specific alkaline phosphatases (TNAPs) can also produce AMP or adenosine directly (Figure 11). This shows that adenosine can be made even if CD39 or CD73 are not active (Yang et al., 2025, Tozaki-Saitoh et al., 2022). In mouse model experiments, adenosine production still occurred even after CD39 was knocked out, suggesting that other pathways can also generate adenosine (Wang et al., 2020).

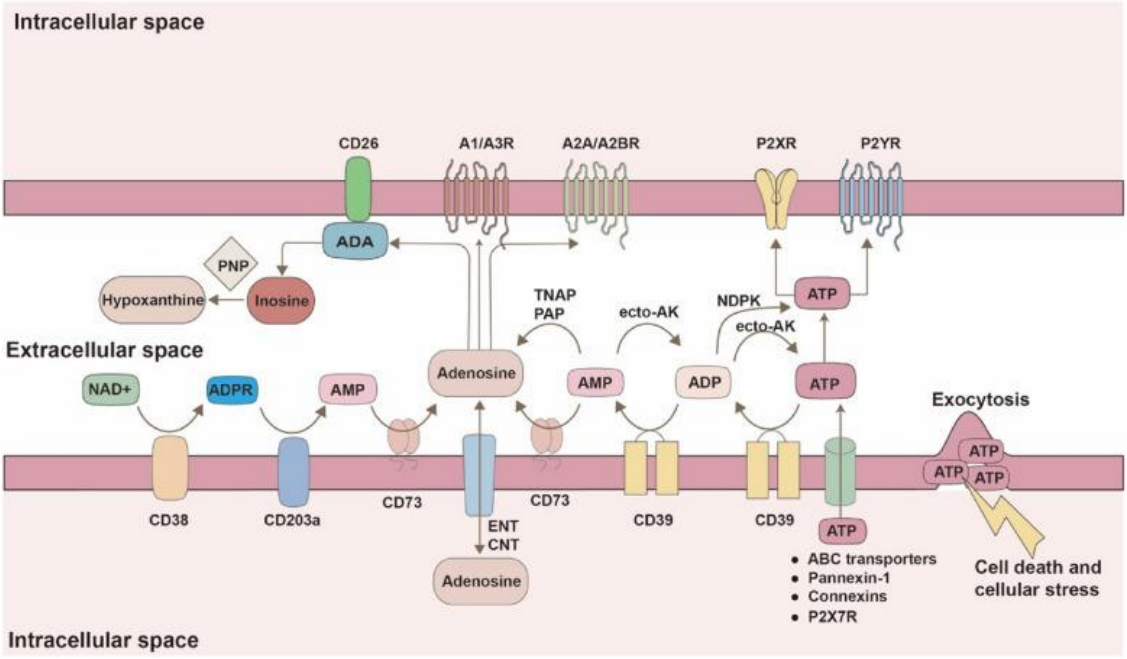

Figure 11. Adenosine production pathways in the tumor microenvironment. (Yang et al., 2025)

ATP can be converted to adenosine mainly via the CD39-CD73 pathway, while alternative pathways such as CD38-CD203a-CD73 and membrane-bound phosphatases (TNAP, PAP) also contribute.

Even though our experiments with CD39 knockout did not produce the expected results, existing research shows that CD39 remains an important target in cancer immunotherapy. Many studies have found that CD39 can weaken immune responses triggered by chemotherapy, and blocking CD39 can help improve treatment by maintaining higher ATP levels in the tumor environment. Brauneck et al. from our group also showed that blocking CD39 with the nanobody SB24 enhanced T cell proliferation and cytotoxicity. (Yin et al., 2025, Warren et al., 2023, Brauneck et al., 2024). This suggests that, despite our negative findings, continuing to explore CD39 inhibition is worthwhile and may still offer valuable therapeutic opportunities.

6. Conclusion

This study explored acute leukemia from two main directions. The first part focused on improving the electroporation conditions in AML cell lines, with the goal of establishing stable knockout models for later immunology-related research. The second part explored the function of CD39 in AML cells.

The main findings are as follows.

1. For all three AML cell lines used in this work (MOLM-13, OCI-AML5, and TF-1), the best electroporation condition was the same. A setting of 150 V for 5 ms gave the most suitable balance between transfection efficiency and cell survival.
2. By applying these optimized conditions to CRISPR-Cas9 RNP delivery, we identified an effective protocol for generating knockout cells. The mixture containing 37.5 pmol Cas9 and 75 pmol sgRNA resulted in the highest protein knockout level.

3. CRISPR-Cas9 knocked out CD48 in OCI-AML5 cells in a dose dependent way. Flow cytometry and on-target sequencing showed consistent results. No off-target effects were detected. CD39 was completely knocked out and confirmed by flow cytometry and sequencing.

4. Using the CD39 knockout cell lines, we carried out functional experiments. The results showed that loss of CD39 did not reduce tumor cell growth and did not make AML cells more sensitive to T cell mediated killing.

These findings not only improved current methods for generating stable knockout models, but also laid a solid foundation for future functional studies.

However, this study also has several limitations. Electroporation in primary leukemia cells was not successful. As the CD39 knockout was only in AML cells, effects in immune cells could not be evaluated. Therefore, testing additional AML cell lines and applying different approaches, such as using CD39 inhibitors, would allow a more comprehensive comparison. This would help to further clarify the role of CD39 in AML. And we only tested two predicted off-target sites, ASXL3 and RAB4B, out of the five predicted by CRISPOR software. These limitations highlight directions for future work, including improving gene-editing efficiency in primary cells, expanding the range of model systems to better understand the function of CD39 in AML and evaluating off-target editing efficiency fully.

7. Summary

7.1 Summary in English

Immunotherapy plays a crucial role in the treatment of acute leukemia. In recent years, various new drugs have been developed for this disease. However, leukemia cells frequently develop to drug resistance, which makes it necessary to continuously explore new immune targets as potential backup treatment options (Restelli et al., 2024). Suspension cells, such as leukemia cells, are generally difficult to transfect (Tang et al., 2018). Therefore, we began exploring how to achieve efficient and reproducible electroporation in AML cell lines. This work aimed to provide an experimental foundation for subsequent studies on immune targets. We introduced GFP mRNA into MOLM-13, OCI-AML5, and TF-1 cell lines by electroporation and tested six different electroporation conditions: 100 V 5 ms, 100 V 10 ms, 150 V 5 ms, 150 V 10 ms, 200 V 5 ms, and 200 V 10 ms. Flow cytometry analysis showed that 150 V at 5 ms gave the best results. To further investigate the roles of various target proteins in AML cell lines and compare the electroporation efficiency, we tested three different concentration combinations of Cas9 and sgRNA: 7.5 pmol Cas9 with 7.5 pmol sgRNA, 37.5 pmol Cas9 with 37.5 pmol sgRNA, and 37.5 pmol Cas9 with 75 pmol sgRNA. We knocked out CD111 and CD48 in OCI-AML5 cells, CD111 in MOLM-13 cells, respectively. Consistently, the RNP combination of 37.5 pmol Cas9 and 75 pmol sgRNA produced the highest protein knockout rates, which were 46.7%, 62.4%, and 31.4%, respectively. All the cell lines listed in Table 6 were generated by using electroporation combined with CRISPR-Cas9 to establish stable protein knockout cell lines. After successfully establishing the CD39 knockout cell line, I performed related functional experiments, including proliferation assays and tumor killing assays. Unfortunately, the results showed that knocking out CD39 did not inhibit tumor cell proliferation nor increase their sensitivity to T cell–mediated killing.

7.2 Zusammenfassung

Die Immuntherapie spielt eine wichtige Rolle bei der Behandlung der akuten Leukämie. In den letzten Jahren wurden verschiedene neue Medikamente für diese Erkrankung entwickelt. Leukämiezellen neigen jedoch zu Medikamentenresistenzen, weshalb es notwendig ist, ständig neue Immunziele als mögliche Backup-Behandlungsoptionen zu untersuchen (Restelli et al., 2024). Suspensionenzellen wie Leukämiezellen sind generell schwer zu transfizieren (Tang et al., 2018). Daher begannen wir zu erforschen, wie man eine effiziente und reproduzierbare Elektroporation in AML-Zelllinien erreichen kann, um eine experimentelle Grundlage für spätere Studien zu Immunzielen zu schaffen. Wir führten GFP-mRNA mittels Elektroporation in die Zelllinien MOLM-13, OCI-AML5 und TF-1 ein und testeten sechs Elektroporationsbedingungen: 100 V 5 ms, 100 V 10 ms, 150 V 5 ms, 150 V 10 ms, 200 V 5 ms und 200 V 10 ms. Die Durchflusszytometrie zeigte, dass 150 V und 5 ms die besten Ergebnisse lieferten. Um die Rolle verschiedener Zielproteine in AML-Zelllinien weiter zu untersuchen, testeten wir drei Konzentrationskombinationen von Cas9 und sgRNA: 7,5 pmol Cas9 mit 7,5 pmol sgRNA, 37,5 pmol Cas9 mit 37,5 pmol sgRNA und 37,5 pmol Cas9 mit 75 pmol sgRNA, und verglichen deren Effizienz beim Protein-Knockout. Wir führten einen Knockout von CD111 und CD48 in OCI-AML5-Zellen sowie von CD111 in MOLM-13-Zellen durch. Konsistent erzielte die Kombination aus 37,5 pmol Cas9 und 75 pmol sgRNA die höchsten Knockout-Raten von 46.7%, 62.4%, and 31.4%. Alle in Tabelle 6 aufgeführten Zelllinien wurden von mir durch Elektroporation zusammen mit CRISPR-Cas9 erzeugt, um stabile Protein-Knockout-Zelllinien herzustellen. Nach der erfolgreichen Herstellung der CD39-Knockout-Zelllinie führte ich funktionelle Experimente durch, darunter Proliferationsassays und Tumor-Kill-Assays. Leider zeigten die Ergebnisse, dass der Knockout von CD39 weder das Tumorzellwachstum hemmte noch die Empfindlichkeit gegenüber T-Zell-vermitteltem Zellabtöten erhöhte.

8. References

ABD EL-FATTAH, E. E. & SELIM, H. M. 2022. Reprograming immune microenvironment modulates CD47 cancer stem cells in hepatocellular carcinoma. *Int Immunopharmacol,* 113**,** 109475.

AGARWAL, A. & TYNER, J. W. 2016. RNAi Screening of Leukemia Cells Using Electroporation. *Methods Mol Biol,* 1470**,** 85-94.

AHVATI, H., ROUDI, R., SOBHANI, N. & SAFARI, F. 2025. CD47 as a potent target in cancer immunotherapy: A review. *Biochim Biophys Acta Rev Cancer,* 1880**,** 189294.

ALAWAR, N., SCHIRRA, C., HOHMANN, M. & BECHERER, U. 2024. A solution for highly efficient electroporation of primary cytotoxic T lymphocytes. *BMC Biotechnology,* 24**,** 16.

AROUA, N., BOET, E., GHISI, M., NICOLAU-TRAVERS, M. L., SALAND, E., GWILLIAM, R., DE TONI, F., HOSSEINI, M., MOUCHEL, P. L., FARGE, T., BOSC, C., STUANI, L., SABATIER, M., MAZED, F., LARRUE, C., JARROU, L., GANDARILLAS, S., BARDOTTI, M., PICARD, M., SYRYKH, C., LAURENT, C., GOTANèGRE, M., BONNEFOY, N., BELLVERT, F., PORTAIS, J. C., NICOT, N., AZUAJE, F., KAOMA, T., JOFFRE, C., TAMBURINI, J., RéCHER, C., VERGEZ, F. & SARRY, J. E. 2020. Extracellular ATP and CD39 Activate cAMP-Mediated Mitochondrial Stress Response to Promote Cytarabine Resistance in Acute Myeloid Leukemia. *Cancer Discov,* 10**,** 1544-1565.

BAJWA, K. K., PUNETHA, M., KUMAR, D., YADAV, P. S., LONG, C. R. & SELOKAR, N. L. 2023. Electroporation-based CRISPR gene editing in adult buffalo fibroblast cells. *Anim Biotechnol,* 34**,** 5055-5066.

BAREKE, H., JUANES-VELASCO, P., LANDEIRA-VIñUELA, A., HERNANDEZ, A. P., CRUZ, J. J., BELLIDO, L., FONSECA, E., NIEBLA-CáRDENAS, A., MONTALVILLO, E., GóNGORA, R. & FUENTES, M. 2021. Autoimmune Responses in Oncology: Causes and Significance. *Int J Mol Sci,* 22.

BASTID, J., REGAIRAZ, A., BONNEFOY, N., DEJOU, C., GIUSTINIANI, J., LAHEURTE, C., COCHAUD, S., LAPREVOTTE, E., FUNCK-BRENTANO, E., HEMON, P., GROS, L., BEC, N., LARROQUE, C., ALBERICI, G., BENSUSSAN, A. & ELIAOU, J. F. 2015. Inhibition of CD39 enzymatic function at the surface of tumor cells alleviates their immunosuppressive activity. *Cancer Immunol Res,* 3**,** 254-65.

BEHR, M., ZHOU, J., XU, B. & ZHANG, H. 2021. In vivo delivery of CRISPR-Cas9 therapeutics: Progress and challenges. *Acta Pharm Sin B,* 11**,** 2150-2171.

BELAALOUI, G., IMBERT, A. M., BARDIN, F., TONNELLE, C., DUBREUIL, P., LOPEZ, M. & CHABANNON, C. 2003. Functional characterization of human CD34+ cells that express low or high levels of the membrane antigen CD111 (nectin 1). *Leukemia,* 17**,** 1137-45.

BEXTE, T., ALZUBI, J., REINDL, L. M., WENDEL, P., SCHUBERT, R., SALZMANN-MANRIQUE, E., VON METZLER, I., CATHOMEN, T. & ULLRICH, E. 2022. CRISPR-Cas9 based gene editing of the immune checkpoint NKG2A enhances NK cell mediated cytotoxicity against multiple myeloma. *Oncoimmunology,* 11**,** 2081415.

BRAUNECK, E., LEONHARDT, L. G., ASSEMISSEN, A. M., WAHID, Y., KRUPPA, M., KRUPPA, N., KRUGER, J., MENZEL, S., KOCH-NOLTE, F., KYLIES, J., WEISEL, K., BOKEMEYER, C., WELLBROCK, J., FIEDLER, W., VIEZENS, L. & BRAUNECK, F. 2025. Expression of the TIGIT axis and the CD39/CD73 purinergic pathway in bone metastasis-derived immune cells. *Cancer Immunol Immunother,* 74**,** 182.

BRAUNECK, F., FISCHER, B., WITT, M., MUSCHHAMMER, J., OELRICH, J., DA COSTA AVELAR, P. H., TSOKA, S., BULLINGER, L., SEUBERT, E., SMIT, D. J., BOKEMEYER, C., ACKERMANN, C., WELLBROCK, J., HAAG, F. & FIEDLER, W. 2022. TIGIT blockade repolarizes AML-associated TIGIT(+) M2 macrophages to an M1 phenotype and increases CD47-mediated phagocytosis. *J Immunother Cancer,* 10.

BRAUNECK, F., MENZEL, S., KRUPPA, N., KOCH-NOLTE, F., FIEDLER, W. & WELLBROCK, J. 2024. CD39 Is Predominantly Expressed in Adverse AML Patients and Blockade By a New Anti-CD39 Nanobody Increases Lysis of AML Blasts. *Blood,* 144**,** 1397-1397.

BRAUNECK, F., SEUBERT, E., WELLBROCK, J., SCHULZE ZUR WIESCH, J., DUAN, Y., MAGNUS, T., BOKEMEYER, C., KOCH-NOLTE, F., MENZEL, S. & FIEDLER, W. 2021. Combined Blockade of TIGIT and CD39 or A2AR Enhances NK-92 Cell-Mediated Cytotoxicity in AML. *Int J Mol Sci,* 22.

BREES, C. & FRANSEN, M. 2014. A cost-effective approach to microporate mammalian cells with the Neon Transfection System. *Anal Biochem,* 466**,** 49-50.

BRUCK, O., DUFVA, O., HOHTARI, H., BLOM, S., TURKKI, R., ILANDER, M., KOVANEN, P., PALLAUD, C., RAMOS, P. M., LAHTEENMAKI, H., VALIMAKI, K., EL MISSIRY, M., RIBEIRO, A., KALLIONIEMI, O., PORKKA, K., PELLINEN, T. & MUSTJOKI, S. 2020.

Immune profiles in acute myeloid leukemia bone marrow associate with patient age, T-cell receptor clonality, and survival. *Blood Adv,* 4**,** 274-286.

CANNONS, J. L., TANGYE, S. G. & SCHWARTZBERG, P. L. 2011. SLAM family receptors and SAP adaptors in immunity. *Annu Rev Immunol,* 29**,** 665-705.

CATALáN, R., OROZCO-MORALES, M., HERNáNDEZ-PEDRO, N. Y., GUIJOSA, A., COLíN-GONZáLEZ, A. L., ÁVILA-MORENO, F. & ARRIETA, O. 2020. CD47-SIRPα Axis as a Biomarker and Therapeutic Target in Cancer: Current Perspectives and Future Challenges in Nonsmall Cell Lung Cancer. *J Immunol Res,* 2020**,** 9435030.

CEMAZAR, M., SERSA, G., WILSON, J., TOZER, G. M., HART, S. L., GROSEL, A. & DACHS, G. U. 2002. Effective gene transfer to solid tumors using different nonviral gene delivery techniques: electroporation, liposomes, and integrin-targeted vector. *Cancer Gene Ther,* 9**,** 399-406.

CHEHELGERDI, M., CHEHELGERDI, M., KHORRAMIAN-GHAHFAROKHI, M., SHAFIEIZADEH, M., MAHMOUDI, E., ESKANDARI, F., RASHIDI, M., ARSHI, A. & MOKHTARI-FARSANI, A. 2024. Comprehensive review of CRISPR-based gene editing: mechanisms, challenges, and applications in cancer therapy. *Mol Cancer,* 23**,** 9.

CHENG, Q., XIA, J., WANG, K., ZHANG, Y., CHEN, Y., ZHONG, Q., WANG, X. & WU, Q. 2022. CRISPR/Cas9 ribonucleoprotein (RNP) complex enables higher viability of transfected cells in genome editing of acute myeloid cells. *Ann Transl Med,* 10**,** 862.

CHICAYBAM, L., BARCELOS, C., PEIXOTO, B., CARNEIRO, M., LIMIA, C. G., REDONDO, P., LIRA, C., PARAGUASSú-BRAGA, F., VASCONCELOS, Z. F., BARROS, L. & BONAMINO, M. H. 2016. An Efficient Electroporation Protocol for the Genetic Modification of Mammalian Cells. *Front Bioeng Biotechnol,* 4**,** 99.

COVELLO, G., SIVA, K., ADAMI, V. & DENTI, M. A. 2014. An electroporation protocol for efficient DNA transfection in PC12 cells. *Cytotechnology,* 66**,** 543-53.

DANECEK, P., BONFIELD, J. K., LIDDLE, J., MARSHALL, J., OHAN, V., POLLARD, M. O., WHITWHAM, A., KEANE, T., MCCARTHY, S. A., DAVIES, R. M. & LI, H. 2021. Twelve years of SAMtools and BCFtools. *Gigascience,* 10.

DELTEIL, C., TEISSIE, J. & ROLS, M. P. 2000. Effect of serum on in vitro electrically mediated gene delivery and expression in mammalian cells. *Biochim Biophys Acta,* 1467**,** 362-8.

DESBIOLLES, B. X. E., DE COULON, E., MAïNO, N., BERTSCH, A., ROHR, S. & RENAUD, P. 2020. Nanovolcano microelectrode arrays: toward long-term on-demand registration of transmembrane action potentials by controlled electroporation. *Microsyst Nanoeng,* 6**,** 67.

DEVIREDDY, L. R., MYERS, M., SCREVEN, R., LIU, Z. & BOXER, L. 2019. A serum-free medium formulation efficiently supports isolation and propagation of canine adipose-derived mesenchymal stem/stromal cells. *PLoS One,* 14**,** e0210250.

ENSSLE, S., SAX, A., MAY, P., EL KHAWANKY, N., SOLIMAN, N., PERL, M., ENSSLE, J. C., KREY, K., RULAND, J., PICHLMAIR, A., BASSERMANN, F., POECK, H. & HEIDEGGER, S. 2025. Gasdermin E links tumor cell-intrinsic nucleic acid signaling to proinflammatory cell death for successful checkpoint inhibitor cancer immunotherapy. *Oncoimmunology,* 14**,** 2504244.

ESFAHANI, K., ROUDAIA, L., BUHLAIGA, N., DEL RINCON, S. V., PAPNEJA, N. & MILLER, W. H., JR. 2020. A review of cancer immunotherapy: from the past, to the present, to the future. *Curr Oncol,* 27**,** S87-S97.

FENG, L., SUN, X., CSIZMADIA, E., HAN, L., BIAN, S., MURAKAMI, T., WANG, X., ROBSON, S. C. & WU, Y. 2011. Vascular CD39/ENTPD1 directly promotes tumor cell growth by scavenging extracellular adenosine triphosphate. *Neoplasia,* 13**,** 206-16.

FENG, Y., SASSI, S., SHEN, J. K., YANG, X., GAO, Y., OSAKA, E., ZHANG, J., YANG, S., YANG, C., MANKIN, H. J., HORNICEK, F. J. & DUAN, Z. 2015. Targeting CDK11 in osteosarcoma cells using the CRISPR-Cas9 system. *J Orthop Res,* 33**,** 199-207.

FREISLEBEN, F., BEHRMANN, L., THADEN, V., MUSCHHAMMER, J., BOKEMEYER, C., FIEDLER, W. & WELLBROCK, J. 2020. Downregulation of GLI3 Expression Mediates Chemotherapy Resistance in Acute Myeloid Leukemia. *Int J Mol Sci,* 21.

FRIEDMAN, G. K., MOORE, B. P., NAN, L., KELLY, V. M., ETMINAN, T., LANGFORD, C. P., XU, H., HAN, X., MARKERT, J. M., BEIERLE, E. A. & GILLESPIE, G. Y. 2016. Pediatric medulloblastoma xenografts including molecular subgroup 3 and CD133+ and CD15+ cells are sensitive to killing by oncolytic herpes simplex viruses. *Neuro Oncol,* 18**,** 227-35.

GOLBERG, A., BRUINSMA, B. G., JARAMILLO, M., YARMUSH, M. L. & UYGUN, B. E. 2016. Rat liver regeneration following ablation with irreversible electroporation. *PeerJ,* 4**,** e1571.

GUO, S., HAN, F. & ZHU, W. 2022. CD39 - A bright target for cancer immunotherapy. *Biomed Pharmacother,* 151**,** 113066.

HAN, Y., LEE, T., HE, Y., RAMAN, R., IRIZARRY, A., MARTIN, M. L. & GIACCONE, G. 2022. The regulation of CD73 in non-small cell lung cancer. *Eur J Cancer,* 170**,** 91-102.

HäUSLER, S. F., MONTALBáN DEL BARRIO, I., STROHSCHEIN, J., CHANDRAN, P. A., ENGEL, J. B., HöNIG, A., OSSADNIK, M., HORN, E., FISCHER, B., KROCKENBERGER, M., HEUER, S., SEIDA, A. A., JUNKER, M., KNEITZ, H., KLOOR, D., KLOTZ, K. N., DIETL, J. & WISCHHUSEN, J. 2011. Ectonucleotidases CD39 and CD73 on OvCA cells are potent adenosine-generating enzymes responsible for adenosine receptor 2A-dependent suppression of T cell function and NK cell cytotoxicity. *Cancer Immunol Immunother,* 60**,** 1405-18.

HAYES, G. M., CAIRNS, B., LEVASHOVA, Z., CHINN, L., PEREZ, M., THEUNISSEN, J. W., LIAO-CHAN, S., BERMUDEZ, A., FLORY, M. R., SCHWEIGHOFER, K. J. & E, H. V. D. H. 2015. CD39 is a promising therapeutic antibody target for the treatment of soft tissue sarcoma. *Am J Transl Res,* 7**,** 1181-8.

HEGAZY, G. E., ABU-SERIE, M. M., ABOU-ELELA, G. M., GHOZLAN, H., SABRY, S. A., SOLIMAN, N. A., TELEB, M. & ABDEL-FATTAH, Y. R. 2022. Bioprocess development for biosurfactant production by Natrialba sp. M6 with effective direct virucidal and anti-replicative potential against HCV and HSV. *Sci Rep,* 12**,** 16577.

HOSEN, N., ICHIHARA, H., MUGITANI, A., AOYAMA, Y., FUKUDA, Y., KISHIDA, S., MATSUOKA, Y., NAKAJIMA, H., KAWAKAMI, M., YAMAGAMI, T., FUJI, S., TAMAKI, H., NAKAO, T., NISHIDA, S., TSUBOI, A., IIDA, S., HINO, M., OKA, Y., OJI, Y. & SUGIYAMA, H. 2012. CD48 as a novel molecular target for antibody therapy in multiple myeloma. *Br J Haematol,* 156**,** 213-24.

HRYHOROWICZ, M., LIPINSKI, D., ZEYLAND, J. & SLOMSKI, R. 2017. CRISPR/Cas9 Immune System as a Tool for Genome Engineering. *Arch Immunol Ther Exp (Warsz),* 65**,** 233-240.

HUANG, S., APASOV, S., KOSHIBA, M. & SITKOVSKY, M. 1997. Role of A2a extracellular adenosine receptor-mediated signaling in adenosine-mediated inhibition of T-cell activation and expansion. *Blood,* 90**,** 1600-10.

HYDER, I., EGHBALSAIED, S. & KUES, W. A. 2020. Systematic optimization of square-wave electroporation conditions for bovine primary fibroblasts. *BMC Mol Cell Biol,* 21**,** 9.

JANIK, E., NIEMCEWICZ, M., CEREMUGA, M., KRZOWSKI, L., SALUK-BIJAK, J. & BIJAK, M. 2020. Various Aspects of a Gene Editing System-CRISPR-Cas9. *Int J Mol Sci,* 21.

KANG, S., KIM, K. H. & KIM, Y. C. 2015. A novel electroporation system for efficient molecular delivery into Chlamydomonas reinhardtii with a 3-dimensional microelectrode. *Sci Rep,* 5**,** 15835.

KCIUK, M., YAHYA, E. B., MOHAMED IBRAHIM MOHAMED, M., RASHID, S., IQBAL, M. O., KONTEK, R., ABDULSAMAD, M. A. & ALLAQ, A. A. 2023. Recent Advances in Molecular Mechanisms of Cancer Immunotherapy. *Cancers (Basel),* 15.

KRUGER, J., WELLBROCK, J., WITT, M., KRUPPA, N., MUSCHHAMMER, J., BOKEMEYER, C., MODEMANN, F., FIEDLER, W., BEHRMANN, L. & BRAUNECK, F. 2024. Murine Regulatory CD4(+) T Cells Are Increased in Leukemic Spleens and Show High Co-Expression of Co-Regulatory Molecules CD39, CD73, PD1, and TIGIT. *Int J Mol Sci,* 25.

LEE, D. H., KANG, S. H., CHOI, D. S., KO, M., CHOI, E., AHN, H., MIN, H., OH, S. J., LEE, M. S., PARK, Y. & JIN, H. S. 2021. Genome wide CRISPR screening reveals a role for sialylation in the tumorigenesis and chemoresistance of acute myeloid leukemia cells. *Cancer Lett,* 510**,** 37-47.

LI, H. & DURBIN, R. 2010. Fast and accurate long-read alignment with Burrows-Wheeler transform. *Bioinformatics,* 26**,** 589-95.

LI, S., CHEN, D., YANG, Y., GUO, H., LIU, D., SUN, N., BAI, X., WANG, K., LI, T., LI, G., YANG, C., ZHANG, W., ZHANG, L., ZHAO, G., PENG, L., LIU, S., TU, X., ZHANG, R. & TIAN, W. 2024. Combining CD38 antibody with CD47 blockade is a promising strategy for treating hematologic malignancies expressing CD38. *Front Immunol,* 15**,** 1398508.

LIU, Y., LI, Z., ZHAO, X., XIAO, J., BI, J., LI, X. Y., CHEN, G. & LU, L. 2023. Review immune response of targeting CD39 in cancer. *Biomark Res,* 11**,** 63.

LIU, Y., WENG, L., WANG, Y., ZHANG, J., WU, Q., ZHAO, P., SHI, Y., WANG, P. & FANG, L. 2024. Deciphering the role of CD47 in cancer immunotherapy. *J Adv Res,* 63**,** 129-158.

MARTIN, T. A., LANE, J., HARRISON, G. M. & JIANG, W. G. 2013. The expression of the Nectin complex in human breast cancer and the role of Nectin-3 in the control of tight junctions during metastasis. *PLoS One,* 8**,** e82696.

MCARDEL, S. L., TERHORST, C. & SHARPE, A. H. 2016. Roles of CD48 in regulating immunity and tolerance. *Clin Immunol,* 164**,** 10-20.

MOESTA, A. K., LI, X. Y. & SMYTH, M. J. 2020. Targeting CD39 in cancer. *Nat Rev Immunol,* 20**,** 739-755.

MOHAMED JIFFRY, M. Z., KLOSS, R., AHMED-KHAN, M., CARMONA-PIRES, F., OKAM, N., WEERADDANA, P., DHARMARATNA, D., DANDWANI, M. & MOIN, K. 2023. A review of treatment options employed in relapsed/refractory AML. *Hematology,* 28**,** 2196482.

MOHAMMADIAN GOL, T., KIM, M., SINN, R., UREñA-BAILéN, G., STEGMEYER, S., GRATZ, P. G., ZAHEDIPOUR, F., ROIG-MERINO, A., ANTONY, J. S. & MEZGER, M. 2023. CRISPR-Cas9-Based Gene Knockout of Immune Checkpoints in Expanded NK Cells. *Int J Mol Sci,* 24.

MONTERO, E. & ISENBERG, J. S. 2023. The TSP1-CD47-SIRPα interactome: an immune triangle for the checkpoint era. *Cancer Immunol Immunother,* 72**,** 2879-2888.

NELDEBORG, S., SOERENSEN, J. F., MOLLER, C. T., BILL, M., GAO, Z., BAK, R. O., HOLM, K., SORENSEN, B., NYEGAARD, M., LUO, Y., HOKLAND, P., STOUGAARD, M., LUDVIGSEN, M. & HOLM, C. K. 2023. Dual intron-targeted CRISPR-Cas9-mediated disruption of the AML RUNX1-RUNX1T1 fusion gene effectively inhibits proliferation and decreases tumor volume in vitro and in vivo. *Leukemia,* 37**,** 1792-1801.

NGUYEN, T. M., JOYCE, P., ROSS, D. M., BREMMELL, K., JAMBHRUNKAR, M., WONG, S. S. & PRESTIDGE, C. A. 2024. Combating Acute Myeloid Leukemia via Sphingosine Kinase 1 Inhibitor-Nanomedicine Combination Therapy with Cytarabine or Venetoclax. *Pharmaceutics,* 16.

OHTA, A. & SITKOVSKY, M. 2001. Role of G-protein-coupled adenosine receptors in downregulation of inflammation and protection from tissue damage. *Nature,* 414**,** 916-20.

PATHAK, N., PATINO, C. A., RAMANI, N., MUKHERJEE, P., SAMANTA, D., EBRAHIMI, S. B., MIRKIN, C. A. & ESPINOSA, H. D. 2023. Cellular Delivery of Large Functional Proteins and Protein-Nucleic Acid Constructs via Localized Electroporation. *Nano Lett,* 23**,** 3653-3660.

PELCOVITS, A. & NIROULA, R. 2020. Acute Myeloid Leukemia: A Review. *R I Med J (2013),* 103**,** 38-40.

POTOČNIK, T., SACHDEV, S., POLAJŽER, T., MAČEK LEBAR, A. & MIKLAVČIČ, D. 2022. Efficient Gene Transfection by Electroporation—In Vitro and In Silico Study of Pulse Parameters. *Applied Sciences,* 12**,** 8237.

QIU, Y., CHEN, T., HU, R., ZHU, R., LI, C., RUAN, Y., XIE, X. & LI, Y. 2021. Next frontier in tumor immunotherapy: macrophage-mediated immune evasion. *Biomark Res,* 9**,** 72.

QUINLAN, A. R. & HALL, I. M. 2010. BEDTools: a flexible suite of utilities for comparing genomic features. *Bioinformatics,* 26**,** 841-2.

RESTELLI, C., RUELLA, M., PARUZZO, L., TARELLA, C., PELICCI, P. G. & COLOMBO, E. 2024. Recent Advances in Immune-Based Therapies for Acute Myeloid Leukemia. *Blood Cancer Discov,* 5**,** 234-248.

RICHTER, F., MAPFUMO, P., MARTIN, L., SOLOMUN, J. I., HAUSIG, F., FRIETSCH, J. J., ERNST, T., HOEPPENER, S., BRENDEL, J. C. & TRAEGER, A. 2021. Improved gene delivery to K-562 leukemia cells by lipoic acid modified block copolymer micelles. *J Nanobiotechnology,* 19**,** 70.

ROMANCZYK, W. & PRYCZYNICZ, A. 2025. The Significance of Nectin Family Proteins in Various Cancerogenous Processes. *Int J Mol Sci,* 26.

SCHAKOWSKI, F., BUTTGEREIT, P., MAZUR, M., MäRTEN, A., SCHöTTKER, B., GORSCHLüTER, M. & SCHMIDT-WOLF, I. G. 2004. Novel non-viral method for transfection of primary leukemia cells and cell lines. *Genet Vaccines Ther,* 2**,** 1.

SHALLIS, R. M., WANG, R., DAVIDOFF, A., MA, X. & ZEIDAN, A. M. 2019. Epidemiology of acute myeloid leukemia: Recent progress and enduring challenges. *Blood Rev,* 36**,** 70-87.

SHIN, H. & MIN, D. H. 2023. Highly Efficient Messenger RNA Transfection of Hard-to-Transfect Cells using Carbon Nanodots. *ACS Omega,* 8**,** 29113-29121.

SHORT, N. J., RYTTING, M. E. & CORTES, J. E. 2018. Acute myeloid leukaemia. *Lancet,* 392**,** 593-606.

SMITH, G. M., BIGGS, J., NORRIS, B., ANDERSON-STEWART, P. & WARD, R. 1997. Detection of a soluble form of the leukocyte surface antigen CD48 in plasma and its elevation in patients with lymphoid leukemias and arthritis. *J Clin Immunol,* 17**,** 502-9.

SOLEIMANI SAMARKHAZAN, H., SHAFIEI, F. S., TAGHINEJAD, Z., MALEKNIA, M., NOORMOHAMADI, H., RAOUFI, A. & NOURI, S. 2025. The AML immune paradox:

decoding escape pathways and pioneering checkpoint, vaccine, and combination strategies. *Clin Exp Med,* 25**,** 240.

STAHL, M. & GOLDBERG, A. D. 2019. Immune Checkpoint Inhibitors in Acute Myeloid Leukemia: Novel Combinations and Therapeutic Targets. *Curr Oncol Rep,* 21**,** 37.

STAMM, H., KLINGLER, F., GROSSJOHANN, E. M., MUSCHHAMMER, J., VETTORAZZI, E., HEUSER, M., MOCK, U., THOL, F., VOHWINKEL, G., LATUSKE, E., BOKEMEYER, C., KISCHEL, R., DOS SANTOS, C., STIENEN, S., FRIEDRICH, M., LUTTEROPP, M., NAGORSEN, D., WELLBROCK, J. & FIEDLER, W. 2018a. Immune checkpoints PVR and PVRL2 are prognostic markers in AML and their blockade represents a new therapeutic option. *Oncogene,* 37**,** 5269-5280.

STAMM, H., WELLBROCK, J. & FIEDLER, W. 2018b. Interaction of PVR/PVRL2 with TIGIT/DNAM-1 as a novel immune checkpoint axis and therapeutic target in cancer. *Mamm Genome,* 29**,** 694-702.

TAMPAKIS, A., TAMPAKI, E. C., NONNI, A., DROESER, R., POSABELLA, A., TSOUROUFLIS, G., KONTZOGLOU, K., PATSOURIS, E., VON FLUE, M. & KOURAKLIS, G. 2019. Nectin-1 Expression in Colorectal Cancer: Is There a Group of Patients with High Risk for Early Disease Recurrence? *Oncology,* 96**,** 318-325.

TANG, X., ALJAHDALI, B., ALASIRI, M., BAMASHMOUS, A., CAO, F., DIBART, S. & SALIH, E. 2018. A method for high transfection efficiency in THP-1 suspension cells without PMA treatment. *Anal Biochem,* 544**,** 93-97.

TERZIYSKA, N., CASTRO ALVES, C., GROISS, V., SCHNEIDER, K., FARKASOVA, K., OGRIS, M., WAGNER, E., EHRHARDT, H., BRENTJENS, R. J., ZUR STADT, U., HORSTMANN, M., QUINTANILLA-MARTINEZ, L. & JEREMIAS, I. 2012. In vivo imaging enables high resolution preclinical trials on patients' leukemia cells growing in mice. *PLoS One,* 7**,** e52798.

TIMPERI, E. & BARNABA, V. 2021. CD39 Regulation and Functions in T Cells. *Int J Mol Sci,* 22.

TOZAKI-SAITOH, H., TAKEDA, H. & INOUE, K. 2022. The Role of Microglial Purinergic Receptors in Pain Signaling. *Molecules,* 27.

TYUMENTSEVA, M., TYUMENTSEV, A. & AKIMKIN, V. 2023. CRISPR/Cas9 Landscape: Current State and Future Perspectives. *Int J Mol Sci,* 24.

UDDIN, F., RUDIN, C. M. & SEN, T. 2020. CRISPR Gene Therapy: Applications, Limitations, and Implications for the Future. *Front Oncol,* 10**,** 1387.

VADEIKIENE, R., JAKSTYS, B., UGENSKIENE, R., SATKAUSKAS, S. & JUOZAITYTE, E. 2022. Systemic Optimization of Gene Electrotransfer Protocol Using Hard-to-Transfect UT-7 Cell Line as a Model. *Biomedicines,* 10.

WANG, C., SUN, C., LI, M., XIA, B., WANG, Y., ZHANG, L., ZHANG, Y., WANG, J., SUN, F., LU, S., ZHU, J., HUANG, J. & ZHANG, Y. 2021a. Novel fully human anti-CD47 antibodies stimulate phagocytosis and promote elimination of AML cells. *J Cell Physiol,* 236**,** 4470-4481.

WANG, X., XING, Z., CHEN, H., YANG, H., WANG, Q. & XING, T. 2022. High expression of nectin-1 indicates a poor prognosis and promotes metastasis in hepatocellular carcinoma. *Front Oncol,* 12**,** 953529.

WANG, Y., COPELAND, J., SHIN, M., CHANG, Y. & VENTON, B. J. 2020. CD73 or CD39 Deletion Reveals Different Mechanisms of Formation for Spontaneous and Mechanically Stimulated Adenosine and Sex Specific Compensations in ATP Degradation. *ACS Chem Neurosci,* 11**,** 919-928.

WANG, Y., ZHANG, C., YAN, M., MA, X., SONG, L., WANG, B., LI, P. & LIU, P. 2024. PD-L1 regulates tumor proliferation and T-cell function in NF2-associated meningiomas. *CNS Neurosci Ther,* 30**,** e14784.

WANG, Z., GUAN, W., WANG, M., CHEN, J., ZHANG, L., XIAO, Y., WANG, L., LI, Y. & YU, L. 2021b. AML1-ETO inhibits acute myeloid leukemia immune escape by CD48. *Leuk Lymphoma,* 62**,** 937-943.

WANG, Z., HE, L., LI, W., XU, C., ZHANG, J., WANG, D., DOU, K., ZHUANG, R., JIN, B., ZHANG, W., HAO, Q., ZHANG, K., ZHANG, W., WANG, S., GAO, Y., GU, J., SHANG, L., TAN, Z., SU, H., ZHANG, Y., ZHANG, C. & LI, M. 2021c. GDF15 induces immunosuppression via CD48 on regulatory T cells in hepatocellular carcinoma. *J Immunother Cancer,* 9.

WARREN, M. C., MATISSEK, S., RAUSCH, M., PANDURO, M., HALL, R. J., DULAK, A., BRENNAN, D., DAS YEKKIRALA, S., KOSEOGLU, S., MASIA, R., YANG, Y., REDDY, N., PRENOVITZ, R., STRAND, J., ZAIDI, T., DEVEREAUX, E., FOISSAC, C. J., STAGG, J., LEE, B. H., HOLLAND, P., PALOMBELLA, V. J. & LAKE, A. C. 2023. SRF617 Is a Potent Inhibitor of CD39 with Immunomodulatory and Antitumor Properties. *Immunohorizons,* 7**,** 366-379.

WITKOWSKA, M. & SMOLEWSKI, P. 2018. Immune Checkpoint Inhibitors to Treat Malignant Lymphomas. *J Immunol Res,* 2018**,** 1982423.

WU, B., ZHONG, C., LANG, Q., LIANG, Z., ZHANG, Y., ZHAO, X., YU, Y., ZHANG, H., XU, F. & TIAN, Y. 2021. Poliovirus receptor (PVR)-like protein cosignaling network: new opportunities for cancer immunotherapy. *J Exp Clin Cancer Res,* 40**,** 267.

WU, G., GUO, S., LUO, Q., WANG, X., DENG, W., OUYANG, G., PU, J. J., LEI, W. & QIAN, W. 2023. Preclinical evaluation of CD70-specific CAR T cells targeting acute myeloid leukemia. *Front Immunol,* 14**,** 1093750.

WU, Y., KUANG, D. M., PAN, W. D., WAN, Y. L., LAO, X. M., WANG, D., LI, X. F. & ZHENG, L. 2013. Monocyte/macrophage-elicited natural killer cell dysfunction in hepatocellular carcinoma is mediated by CD48/2B4 interactions. *Hepatology,* 57**,** 1107-16.

WYSOTA, M., KONOPLEVA, M. & MITCHELL, S. 2024. Novel Therapeutic Targets in Acute Myeloid Leukemia (AML). *Curr Oncol Rep,* 26**,** 409-420.

XIA, C., YIN, S., TO, K. K. W. & FU, L. 2023. CD39/CD73/A2AR pathway and cancer immunotherapy. *Mol Cancer,* 22**,** 44.

XU, J., ZHONG, A., ZHANG, S., CHEN, M., ZHANG, L., HANG, X., ZHENG, J., WU, B., DENG, X., PAN, X., WANG, Z., QI, L., SHI, K., LI, S., WANG, Y., WANG, M., CHEN, X., ZHANG, Q., LIU, P., GALE, R. P., CHEN, C., LIU, Y. & NIU, T. 2023. KMT2D Deficiency Promotes Myeloid Leukemias which Is Vulnerable to Ribosome Biogenesis Inhibition. *Adv Sci (Weinh),* 10**,** e2206098.

YANG, J., WANG, L., BYRNES, J. R., KIRKEMO, L. L., DRIKS, H., BELAIR, C. D., AGUILAR, O. A., LANIER, L. L., WELLS, J. A., FONG, L. & BLELLOCH, R. 2024. PVRL2 Suppresses Antitumor Immunity through PVRIG- and TIGIT-independent Pathways. *Cancer Immunol Res,* 12**,** 575-591.

YANG, Y., ZHU, L., XU, Y., LIANG, L., LIU, L., CHEN, X., LI, H. & LIU, H. 2025. The progress and prospects of targeting the adenosine pathway in cancer immunotherapy. *Biomarker Research,* 13**,** 75.

YIN, X., YANG, Y. & LIU, S. 2025. Cancer immunotherapy by adenosinergic CD39 and CD73 as emerging immune checkpoints. *Discov Oncol,* 16**,** 2153.

YUEN, G., KHAN, F. J., GAO, S., STOMMEL, J. M., BATCHELOR, E., WU, X. & LUO, J. 2017. CRISPR/Cas9-mediated gene knockout is insensitive to target copy number but is

dependent on guide RNA potency and Cas9/sgRNA threshold expression level. *Nucleic Acids Res,* 45**,** 12039-12053.

ZHANG, Y., ZHANG, X., CHENG, C., MU, W., LIU, X., LI, N., WEI, X., LIU, X., XIA, C. & WANG, H. 2017. CRISPR-Cas9 mediated LAG-3 disruption in CAR-T cells. *Front Med,* 11**,** 554-562.

ZHANG, Y. & ZHANG, Z. 2020. The history and advances in cancer immunotherapy: understanding the characteristics of tumor-infiltrating immune cells and their therapeutic implications. *Cell Mol Immunol,* 17**,** 807-821.

9. Supplementary materials

9.1 Sequences for CD48 on-target and off-target analysis

1.CD48

guide: GTACATATGACCGTGGTCTC CGG

Reverse: CCGGAGACCACGGTCATATGTAC

CD48: -300 & +300 bp around Position chr1:160685159-160685181

>hg38_dna range=chr1:160684859-160685481 5'pad=0 3'pad=0 strand=+ repeatMasking=none

GATTTGCTCTTTGGCTCCCCTGACTCACCAAGCACTTGCAGCTTGATCTT

CCATTCTTGCTCATTCCCAGTCTTTTTCAACACCCTCATGATGTAGGTGC

TGTTGTCCTCTTTCTGGACCTTAGAGATGTACAGTGCGCCACTCTGAGGA

TCAAGTCTGACCCTGCCTTTAAATTTGGATTCAAAGTACTTAGATTTTCT

GGAATCCCATTCTACAATCTTCTGGTCGAAAGTATAAAACCAGGTTAGTT

GTTTGTAGTTCTCAGGCAGGCTCTCAGAGATGTTCAGAGTCACGTTGCTG

CCGGAGACCACGGTCATATGTACCAAGTGACCTGCCAATGAGATTCAGAG

TGAGACCTGCGCTAGAGGAGGCAGTGTTGCTGACAGGCCCAGGGTATAGC

CTGGGCTGGTGGAACAGGTGAGAAGGAAGGGATTTCTGCTTAGGAGCAGT

GAGTATGGTTTTCACTGGAGGTCCAGGTCTCCTGCTTAGGAACTCAAGAA

AAGTTGAAGCTTGAAAAGTGGGCATGGGGGAAGGGGATGCTGCTTATAAT

TAATCTAGTACTGTCCCCAGAAAATGAAAGAATTGAGTAAGGCCAACTGA

GGTTGGGCCTGGCTCTCTCCCTT

2.RAB4B

guide: GTACATATGACCGTGGTCTC CGG

off-target: GGACAAATGACCCTGGTCTC AGG

Reverse complementary sequence CCTGAGACCAGGGTCATTTGTCC

CFD Off-target score: 0.306526

MIT Off-target score: 0.68

Position: chr19:40796819-40796841:-

RAB4B: -300 & +300 bp around Position: chr19:40796819-40796841:-

>hg38_dna range=chr19:40796519-40797141 5'pad=0 3'pad=0 strand=+ repeatMasking=none

GGCTGGACAGACCCCGGGGACCCTGCAGGTCACCACACCCTTCTCTTTCA

GCTCACCTGTTCTCCAGGACCAGCCCTGCTGGGGCCCAGGCCCAGGCTCT

GAGAGGCCGTGTCCTAACCTGCCCTGGCCCCGGAGAAGCTACGTTGCCAC

CTGTCCCCCTTCCCTGGCCTGGTGGGGCCTGGCTTTGGGGCAAGACTGAG

CCACGGGGGAAGGGGGAATCCCGTACCTGCTGCTGCTTCCTCTGTCTTGG

CTAACGTCTGTCCCCCTGAACCCCTAACCATACCCCAAGAGCTCCCAAAG

CCTGAGACCAGGGTCATTTGTCCCCAACTCCCCATCTGGCCCTGCTGTTG

CTAGTACCTGTTATTTATTACCTGGAGGCCTGTCCAGCACCCACCCTACC

CCCATAAAGCATTGTTTACACCTGTGTCTTGGCCTCCATTATTGTGAGAT

GGCAGGGAGATGGAAGAGGTCCCTGATGGAAGAATCATGTGTCATGGTGT

TTGGGGGCCTTGTTTCTGTTTTTTTGTTGTTGTTGTTGAGATGGAGTTTC

CTTCTTGTTGCCCAGGCTGGAGTGCAGTGGCGTGATCTTGGCTCACCACA

ACCTCCACCTCCCGGGTTCAAGC

3. **ASXL3:**

guide: GTACATATGACCGTGGTCTC *CGG*

off-target: CTACATATGCCCGTGGACTG TGG

Reverse complementary sequence CCACAGTCCACGGGCATATGTAG

CFD Off-target score: 0.007470

MIT Off-target score: 0.25

Position: chr18:33746056-33746078:-

ASXL3: -300 & +300 bp around Position: chr18:33746056-33746078:-

>hg38_dna range=chr18:33745756-33746378 5'pad=0 3'pad=0 strand=+ repeatMasking=none

AAGGGATTGGGAGAGGTTAGTCTTTCCTCAGCACCTCACCAGCTAAGGTT

AGCCAACATGTTATCCCCCAATATGCCCATGAAAGAAGGTGATGAGGTGG

GAGGCACTGCACACACAATGCCAAACAAAGCACTAGTACATCCGCCGCCG

CCACCGCCTCCCCCTCCCCCTCCACCCTTGGCTTTGCCCCCGCCTCCCCC

CCCACCACCTCCGCTACCTCCACCTCTCCCTAATGCAGAAGTCCCATCTG

ATCAAAAACAACCTCCAGTTACCATGGAAACCACTAAGAGACTTAGTTGG

CCACAGTCCACGGGCATATGTAGCAATATAAAATCGGAACCTCTTTCTTT

TGAGGAAGGTTTAAGCAGCAGCTGTGAACTGGGCATGAAACAAGTTTCCT

ATGACCAGAATGAAATGAAAGAACAGTTAAAAGCATTCGCGCTAAAAAGT

GCAGATTTCTCTTCCTATTTGCTTTCTGAGCCACAAAAGCCTTTTACCCA

ATTAGCTGCTCAGAAAATGCAGGTGCAGCAACAACAGCAGCTCTGTGGAA

ATTATCCAACAATACACTTTGGTAGCACGAGTTTCAAAAGGGCAGCATCT

GCAATTGAAAAGTCCATTGGGAT

9.2 Ethics approval document

ETHIK-KOMMISSION DER
ÄRZTEKAMMER
HAMBURG
Körperschaft des öffentlichen Rechts

Ärztekammer Hamburg · Postfach 76 01 09 · 22051 Hamburg

Herrn
Prof. Dr. med. Walter Fiedler
II Med. Klinik und Poliklinik
Onkologisches Zentrum
Universitätsklinikum Hamburg-Eppendorf
Martinistr. 52
20246 Hamburg

17.06.2010

Bearb.-Nr.: **PV3469 (Bitte stets angeben!)**
Studie: Antrag auf Genehmigung zum Aufbau einer Biomaterialbank für die wissenschaftliche Erforschung der akuten myeloischen Leukämie

Sehr geehrter Herr Kollege Fiedler,

über Ihr oben bezeichnetes, zur Primärberatung vorgelegtes Projekt hat die Ethik-Kommission ausführlich beraten.

Das Vorhaben entspricht den berufsrechtlichen bzw. gesetzlichen Anforderungen. Die Ethik-Kommission stimmt dem Vorhaben zu.

Die Kommission weist darauf hin, dass die Verantwortung des Versuchsleiters für das Forschungsvorhaben und seine Durchführung durch das obige Votum der Kommission nicht berührt wird.

Sie werden gebeten, die Ethik-Kommission über alle schwerwiegenden oder unerwarteten Ereignisse, die während der Studie auftreten und die die Sicherheit der Studienteilnehmer gefährden, in Verbindung mit Ihrer Stellungnahme zu unterrichten.
Die Kommission geht davon aus, dass die personenbezogenen Daten der Probanden/ Patienten den datenschutzrechtlichen Vorschriften entsprechend behandelt werden.

Die Ethik-Kommission erwartet, dass ihr nach Abschluss des Projektes unaufgefordert ein Abschluss-Bericht übersandt wird (unter Angabe der Bearb.-Nr.), aus dem der Erfolg/Misserfolg der Studie sowie Angaben darüber, ob die Studie abgebrochen oder geändert bzw. ob Regressansprüche geltend gemacht wurden, ersichtlich sind.

Mit verbindlicher Empfehlung
Im Auftrage der Kommission:

Prof. Dr. med. Th. Weber
- Vorsitzender -

P.S. Die Ethik-Kommission arbeitet auf der Grundlage deutschen Rechts und Berufsrechts sowie in Anlehnung an die ICH-GCP

Humboldtstraße 67a · 22083 Hamburg
Telefon 040 / 20 22 99-240 · Fax 040 / 20 22 99-410
ethik@aekhh.de · www.aerztekammer-hamburg.de
Geschäftsführung: Dr. Silke Schrum

Bankverbindung:
Deutsche Apoth. u. Ärztebank, BLZ 300 606 01, Konto-Nr. 000 1346 113
BIC DAAEDEDD, IBAN DE71 3006 0601 000 1346 113

10. List of abbreviations

Abbreviation	Full Term
AML	Acute myeloid leukemia
TIGIT	T cell immunoglobulin and immunoreceptor tyrosine-based inhibitory motif
ITIM	Immunoreceptor tyrosine-based inhibitory motif
SLAM	Signaling lymphocyte activation marker
MM	Multiple myeloma
HCC	Hepatocellular carcinoma
ATP	Adenosine triphosphateinto
ADP	Adenosine diphosphate
cAMP	cyclic adenosine monophosphate
SIRPα	Signal-regulatory protein alpha
RNP	Ribonucleoprotein complex
TME	Tumor microenvironment
PAPs	Prostatic acid phosphatases
TNAPs	Tissue-non-specific alkaline phosphatases
CD39	Nucleoside triphosphate diphosphohydrolase 1, NTPDase1
CD73	Ecto-5′-nucleotidase

11. Manuscript in preparation derived from this dissertation

A manuscript titled “Optimization of electroporation conditions for acute myeloid leukemia cell lines and their application in CRISPR-Cas9 mediated gene knockout” is currently being prepared for submission. The work is largely based on the experimental data and analyses presented in this dissertation.

12. Statement of own contribution

I conducted the experiments described in this thesis, including optimizing GFP mRNA electroporation in AML cell lines (MOLM-13, OCI-AML5, and TF-1), performing CRISPR-Cas9 knockouts of CD111, CD48, and CD39, establishing all stable protein knockout cell lines listed in Table 6, and performing functional assays such as proliferation and immune cell-mediated cytotoxicity assay. I performed all data analysis, prepared the figures, and wrote the thesis. The idea to optimize electroporation of AML cell lines was proposed by me and received strong support from my supervisor. The thesis was written by me and revised under the guidance of my supervisor.

13. Acknowledgements

During my time in the lab, I feel I have gained a lot. First, I would like to thank my supervisor PD Dr. rer. nat. Jasmin Wellbrock for her guidance and support. When I started the CD39 project, she helped me to better understand the direction of the research. In the beginning of my experiments, when I was trying both lentiviral transfection and electroporation in acute leukemia cell lines, I faced many failures. However, she always encouraged me and discussed the problems with me in meetings. After many attempts, we finally achieved a satisfying result. I especially appreciate her warm smile, as well as the calmness and broad knowledge she always showed when facing scientific difficulties. When I became interested in optimizing electroporation conditions for leukemia cell lines and shared this idea with her, she immediately supported me and gave me useful tips on the experimental plan. I was always happy to present new data to her and I really appreciated her patience and feedback.

I would also like to thank Dr. med. Franziska Brauneck, who replied to my MD application so quickly and accepted me into the lab. Whenever I felt confused, she always talked to me openly and helped me find a solution.

I am grateful to Dr. Lea Schwarze for teaching me the electroporation technique with so much patience. I still remember the time when I first did flow cytometry alone and suddenly ran into problems. I happened to meet her in the hallway and told her what had happened, and she helped me without hesitation. I am still very thankful for that.

I would like to thank Prof. Walter Fiedler. His dedication left a deep impression on me. He always replied to emails very quickly and helped me solve problems in time.

I would like to thank the technical staff of the lab, including Gabi Vohwinkel, Jana Muschhammer, and Nadine Felber. Without their help and support in the lab, many experiments would not have been possible.

I would like to thank the MD students Moritz Kruppa, Laura Holzapfel, and Dana Bui. Our discussions during experiments and their encouragement during difficult moments helped me a lot. Working with them made many difficult times easier.

I gratefully acknowledge the support of the Deutsche José Carreras Leukämie-Stiftung (Grant number 14 PSD/2024), which made it possible for me to focus on my research. Without the generous support of PD Dr. rer. nat. Jasmin Wellbrock and Prof. Walter Fiedler, I would not have applied for this scholarship and would not have the opportunity to present my poster in Basel, Switzerland.

Thanks to Patrick Blümke and his team of the High-Throughput Sequencing Technology Platform at Leibniz LIV, Hamburg, Germany, for performing sequencing and analysing the data.

I would like to thank the staff of the Flow Cytometry Department, Regine Thiele, Melanie Lachmann-Schwemm, and Dr. rer. nat. Anne Rissiek. Working with them was always a great experience, and their professional support helped resolve problems very efficiently.

Finally, I would like to thank my family. Without their constant care, love, and support, I would not have been able to persevere and complete my studies while living so far away from my hometown. Especially, I would like to thank my daughter for being my beloved child and my source of strength during my MD time. Her support has meant the world to me.

All these experiences have become a valuable part of my life, and they will inspire me to move forward into the next step.

14. Eidesstattliche Versicherung

Ich versichere ausdrücklich, dass ich die Arbeit selbständig und ohne fremde Hilfe, insbesondere ohne entgeltliche Hilfe von Vermittlungs- und Beratungsdiensten, verfasst, andere als die von mir angegebenen Quellen und Hilfsmittel nicht benutzt und die aus den benutzten Werken wörtlich oder inhaltlich entnommenen Stellen einzeln nach Ausgabe (Auflage und Jahr des Erscheinens), Band und Seite des benutzten Werkes kenntlich gemacht habe. Das gilt insbesondere auch für alle Informationen aus Internetquellen.

Soweit beim Verfassen der Dissertation KI-basierte Tools („Chatbots“) verwendet wurden, versichere ich ausdrücklich, den daraus generierten Anteil deutlich kenntlich gemacht zu haben. Die „Stellungnahme des Präsidiums der Deutschen Forschungsgemeinschaft (DFG) zum Einfluss generativer Modelle für die Text- und Bilderstellung auf die Wissenschaften und das Förderhandeln der DFG“ aus September 2023 wurde dabei beachtet.

Ferner versichere ich, dass ich die Dissertation bisher nicht einem Fachvertreter an einer anderen Hochschule zur Überprüfung vorgelegt oder mich anderweitig um Zulassung zur Promotion beworben habe.

Ich erkläre mich damit einverstanden, dass meine Dissertation vom Dekanat der Medizinischen Fakultät mit einer gängigen Software zur Erkennung von Plagiaten überprüft werden kann.

Datum 06.07.2026 Unterschrift Rui Lu